Nano/Amorphous Materials and Interface Science Symposium

August 7 ~ 8, 2009

Sansa-tei (Tohgatta, Miyagi-zao, Japan)

August 7 (Friday) 【Room: Aoso】

13:00 ~ 13:10 Opening Address
Takashi Goto (IMR, Tohoku University)

(Chair :T. Goto)

13:10 ~ 13:30 Experimental study on strain distribution of a bone model with a dental implant under simulated dental occlusion
Yasuyuki Morita (RIAM, Kyushu University)

13:30 ~ 13:50 Stress analysis of tooth supporting system based on tooth attachment mechanism
Limei REN (RIAM, Kyushu University)

13:50 ~ 14:10 Finete element analyses of the plastic deformation behavior of model materials for tissue and bone application
Hyoung Seop KIM (Dept. Mter. Sci. Eng., POSTECH, Korea)

14:10 ~ 14:30 Adhesion strength of TiO_2 coating by ECR plasma oxidation
Makoto Fujikawa (Div. Adv. Prost. Dent., Tohoku University)

14:30 ~ 14:40 *Break*

(Chair: H. S. Kim)

14:40 ~ 15:20 (*Keynote Lecture*) The dynamic deformation response of a high-strength, high-toughness 10Ni-0.1C steel
K. S. Kumar (Div. Eng., Brown University, USA)

(Chair : Y. Takao)

15:20 ~ 15:40 Evaluation of different surface modifications for implant alloys in vivo
Yuko Suzuki (Div. Adv. Prost. Dent., Tohoku University)

15:40 ~ 16:00 Influence of immediate and early loading on bone metabolic activity around dental implants in rat tibia using high resolution PET scanner
Miou Yamamoto (Div. Adv. Prost. Dent., Tohoku University)

16:00 ~ 16:20 Interface between titanium implant and calcium phosphate thin film fabricated by RF magnetron sputtering
Kyosuke Ueda (Dept. Mater. Process., Tohoku Universityersity)

16:20 ~ 16:40 Surface modifications of pure titanium and cell-material interactions
Zhaoxiang Chen (RIAM, Kyushu University)

16:40 ~ 16:50 Break

(Chair : K. Sasaki)

16:50 ~ 17:10 Intracellular signal transduction during mechano-response in differentiating chondrocytes
Ichiro Takahashi (Sect. Orthodon., Kyushu University)

17:10 ~ 17:30 Biodegradation behaviors of Mg exposed in vitro and in vivo surroundings
Hyun Kwang Seok (KIST, Korea)

17:30 ~ 17:50 Synergetic effect of sandblasted and acid-etched surface and statin on peri-implant osteogenesis
Yasuko Moriyama (Div. Oral Rihabili., Kyushu University)

17:50 ~ 18:10 Characterization of microstructure and mechanical properties of biodegradable PLLA polymer blends with LTI
Vilay Vannaladsaysy (RIAM, Kyushu University)

19:00 ~ 21:00 *Dinner Meeting* 【Room: Zao】

August 8 (Saturday) 【Room: Aoso】

(Chair : O. Suzuki)

9:00 ~ 09:20 Comparative studies of the peri-implant epithelium of rat gingivae between “Step-type” and “Straight-type” implant system
Iku Atsuta (Div. Oral Rihabili., Kyushu University)

9:20 ~ 09:40 Temporal changes in the ultrastructural localization of bone proteins at the bone-titanium interface of rat
Yasunori Ayukawa Kyushu University.

9:40 ~ 10:00 Corrosion behavior of the Japanese cup-yoke-type magnetic attachments
Yukyo Takada（Div. Dent. Biomater., Tohoku University)

10:00 ~ 10:20 Effect of amino acids on Zn-release from Zn-containing OCP
Yoshitomo Honda (Cranio. Func. Eng., Tohoku University)

10:20 ~ 10:40 Development of artificial bone substitute composed of bioactive MegaGen sythetic bone and osteoconductive hyaluronic acid hydrogels
Sei Kwang Hahn (Dept. Mater. Sci. Eng., POSTECH, Korea)

10:40 ~ 10:50 Break

(Chair : T. Akahori)

10:50 ~ 11:10 Tailoring mechanical properties of PLLA-based scaffolds by structural control
Joo-Eon Park (RIAM, Kyushu University)

11:10 ~ 11:30 Biomechanical risk assessment for fully edentulous maxilla with dental implants
Takaaki Arahira (RIAM, Kyushu University)

11:30 ~ 11:50 Detection of bacteria in closed hollow obturators of maxillary prostheses
Yasuhisa Takeuchi Tohoku University. Grad. Sch. Dent.

11:50 ~ 12:10 Porous alginates scaffolds with various contents of octacalcium phosphate (OCP) crystals
Naru Shiraishi (Div. Adv. Prost. Dent., Tohoku University)

12:10 ~ 13:00 *Lunch Break*

(Chair : T. S. Kim)

13:00 ~ 13:20 Mechanical performances of biomedical Ti and Zr system alloys through thermomechanical treatments
Toshikazu Akahori (IMR, Tohoku University)

13:20 ~ 13:40 Dynamic globularization behaivor and bio-mechanical compatibility of Ti-13Nb-13Zr alloy
Chong Soo Lee (Dept. Mater. Sci. Eng., POSTECH, Korea)

13:40 ~ 14:00 Improvement in mechanical properties of spinal implant rod made of Ti-29Nb-13Ta-4.6Zr
Kengo Narita (IMR, Tohoku University)

14:00 ~ 14:20 Precipitates formed in biomedical Co-Cr-Mo alloys with various carbon contents
Shingo Mineta (Dept. Mater. Process., Tohoku Universityersity)

14:20 ~ 14:40 Thermomechanical characterization of bulk metallic glasses
Kwang Seok Lee (Mater. Process. Div., KIMS, Korea)

14:40 ~ 14:50 *Break*

(Chair : H. Kato)

14:50 ~ 15:10 Preparation and Bioactivation of Zr-Al-Co Bulk Metallic Glasses
Takeshi Wada (IMR, Tohoku University)

15:10 ~ 15:30 Metallic Glass Powders as a binder for poly crystalline diamond
Taek-Soo Kim (KITECH, Korea)

15:30 ~ 15:50 Atomistic interpretation on deformation behavior of bulk metallic glasses
Byeong Joo Lee (Dept. Mater. Sci. Eng., POSTECH, Korea)

15:50 ~ 16:10 Mg-Based Bulk Metallic Glass Composite with Ti Fillers
Hideki Oka (IMR, Tohoku University)

16:10 ~ 16:30 Feasibility of NAPs for the reduction in seintering temperature
Hanshin Choi (KITECH, Korea)

16:30 ~ 16:40 Closing Address
Keiich Sasaki (Grad. Sch. Dent., Tohoku University)

Experimental study on strain distribution of a bone model with a dental implant under simulated dental occlusion

Yasuyuki Morita[1], Lihe Qian[1], Mitsugu Todo[1], Yasuyuki Matsushita[2], Masakazu Uchino[3], Kazuo Arakawa[1] and Kiyoshi Koyano[2]

1 *Research Institute for Applied Mechanics, Kyushu University*

2 *Graduate School of Dental Science, Kyushu University*

3 *Fukuoka Industrial Technology Center*

morita@riam.kyushu-u.ac.jp

Introduction

Recently, dental implants have become important in odontotherapy since they dramatically improve a patient's quality of life by restoring the functions of mastication, speech, and sensuousness diminished by lost teeth or periodontium. However, postoperative complications, such as bone resorption and dental implant fracture, can arise from inappropriate treatment. Many studies have examined the role of mechanical problems in these postoperative complications, but due to experimental difficulties, few studies have investigated the strain and stress distributions in bones resulting from placing dental implants. Most such studies have used numerical analyses, such as the finite element method. Experimentally, the photoelasticity technique can be applied to visualize the stress distribution of a photoelastic polymer monolayer. In general, however, bone consists of a bilayer structure comprising cortical and cancellous bone.

Therefore, this study examined sawbones laminated test blocks, which have a structure close to that of bone. Fixtures were implanted in bone models that simulated bilayer cortical and cancellous bone. A cross-sectional surface was exposed by cutting the specimen with a universal milling machine to observe the fixture/bone interface. Then, we analyzed the displacement and strain distributions in the boundary area under simulated dental occlusion conditions using a digital image correlation (DIC) method. In this study, we compared the displacement/strain distributions between osseointegrated implant and unosseointegrated implant specimens. In the unosseointegrated implant specimen, the fixture which is a component of a dental implant did not adhere to the bone model, since it was simply implanted in the model. Then, the interface simulated an immediate-loaded implantology, which has recently come into widespread use, in which the implant does not adhere to bone in the early stage. On the other hand, in the osseointegrated implant specimen, the fixture adhere to the bone model with adhesive.

Experimental Method

Specimen geometry and manufacture method Sawbones laminated test blocks were used as a bone model to simulate actual bilayer bone consisting of cortical and cancellous alveolar bone. The cortical and cancellous bone specimens were made from glass-reinforced epoxy and solid polyurethane, respectively. The mechanical properties of this phantom bone model are similar to those of actual bone [1]. Each specimen measured 40×40×30 mm^3, and the cortical bone was 2 mm thick at both ends. Tapered fixtures (POI EX FINAFIX POI47-14TP-L; JMM Corp.) were used in this study. The maximum outside diameter, total length, and bone-implanted length of this fixture were 4.7 mm, 16 mm, and 14 mm, respectively.

Specimens were constructed in the following manner: Holes were drilled in the bone model block using the drills specified by JMM. The holes were accurately created using a universal milling machine (2MF-U; Hitachi Seiki) to reduce the individual differences among specimens. Then, a fixture was implanted manually in each hole by self-tapping with a tapping wrench with adhesive (6004N; Sumitomo 3M) for osseointegrated implant specimens and without adhesive for unosseointegrated implant speci-

mens. For the specimens with an implanted fixture, the cross-sectional surface was exposed to measure the whole-field displacement distribution.

Specimen preparation A compression test to simulate dental occlusion was performed in the following manner. (i) Random patterns were created on the area to be observed by spraying it with a synthetic resin, pigment, and organic solvent (S05032; Dai Nippon Toryo) for DIC analysis. (ii) The specimen was placed in a tabletop materials tester (EZ Test; Shimadzu), with a load resolution of 0.010 N and a displacement resolution of 10 μm. (iii) A compression load was applied to the top of the fixture. The pre-compression load was –4.0 N to avoid initial rigid-body movement of the specimen. (iv) The compression load, which paralleled the longitudinal axis of the fixture, was increased until it reached –200 N at a crosshead speed of 0.50 mm/min. (v) Load and displacement data were recorded throughout the loading period and digital images of the specimen surface were taken every –10 N during the continuous loading with a charge-coupled device (CCD) camera (D80; Nikon). Each image measured 2600×3900 pixels, and one pixel was equivalent to an area of 4.7×4.7 μm^2. (vi) Vic-2D (Correlated Solutions) analysis software was for the DIC method.

Experimental Results and Discussion

The strain distributions, ε_{xx}, ε_{zz}, and γ_{xz} were acquired from the displacement distribution obtained by the DIC method. The results were shown in Figs. 1 and 2, which represented the strain distributions of the unosseointegrated implant and the osseointegrated implant specimens, respectively. The location of the strain concentrations was almost same in both specimens. The ε_{xx} and γ_{xz} were concentrated in the bone at the tapered area of the fixture. The concentration of the ε_{zz} appeared in the bone at the tip of the fixture. However, the distributions were quite different. The strain distribution of the unosseointegrated implant specimen did not spread widely to the bone area, though the one of the osseointegrated implant specimen spread pretty widely to the bone area. This means that the occlusion force was supported by many bones in the osseointegrated bone specimen, the unosseointegrated specimen was not. The difference was caused by whether the interface between the bone model and the fixture was bonded or not. The maximum strain values in the unosseointegrated implant specimen were higher than in the osseointegrated implant one. The values were (ε_{xx}, ε_{zz}, γ_{xz}) = (-0.6, -5.0, 1.9%) and (-0.3, -1.5, 0.4%), respectively. This might suggest that the unosseointegrated implantology is subject to bone resorption compared to the osseointegrated one.

Acknowledgements

This work was supported by KAKENHI (No.20760072) and the Japanese Ministry of Education, Culture, Sports, Science and Technology, as part of the "Highly-Functional Interfaces Science: Innovation of Biomaterials with Highly Functional Interface to Host and Parasite" project.

Reference

[1] SAWBONES Worldwide Leaders in Orthopaedic and Medical Models, A Division of Pacific Research Laboratories, Inc., (2008), 72-73.

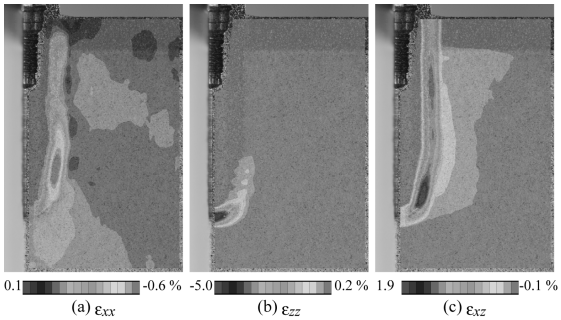

Fig. 1 Strain distributions of an unosseointegrated implant specimen.

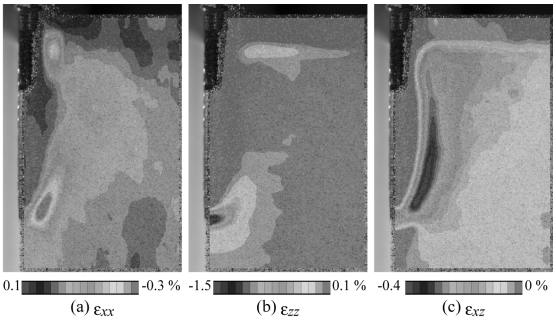

Fig. 2 Strain distributions of an osseointegrated implant specimen.

Stress analysis of tooth supporting system based on detailed attachment mechanism

L.M. Ren, W.X. Wang, Y. Takao, Z.X. Chen

Research Institute for Applied Mechanics, Kyushu University

lmren@riam.kyushu-u.ac.jp

Dental implants have been increasingly used for rehabilitation of the edentulous patients since they were introduced in dentistry. Although successful long-term results of this therapy have been obtained in many clinical situations, some failure rates have been reported. The biologic response of bone to mechanical loads significantly affects implant longevity. Understanding the structure and the mechanical response of biological tissues will provide essential information to engineering materials preparation for replacement due to injury or disease.

In the present study, based on the recently reported theories about the tooth attachment mechanism, multilayered complex finite element models of the tooth and its supporting system were constructed. The effects of the cementum-dentine junction (CDJ) and cementum on the mechanical responses of the tooth supporting system were analyzed. In addition, stress distribution in alveolar bone of natural tooth with the CDJ and cementum were compared with the case of a dental implant. As a major result of this study, it can be stated that the function of the CDJ and cementum is as a cushion pad decreasing the stress of the periodontium under loading forces. Stress levels are greater in the structures without CDJ and cementum than the case with CDJ and cementum. However, most of the reported numerical research did not take CDJ and cementum into account, which possibly resulted in overestimated stress values in the periodontium. From a developing biology perspective, the results of this study provide guidance for the design of dental implants and subsequently improve clinical outcomes.

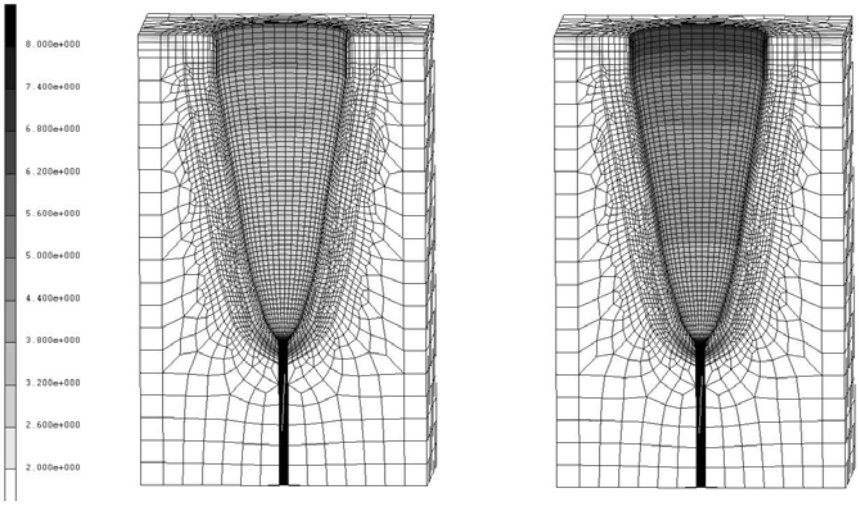

Von Mises stress contours in the tooth supporting structure with CDJ and cementum (left) and without CDJ and cementum (right). High stress concentrations are present at the alveolar crest and root apex.

Finite element analyses on the plastic deformation behavior of model materials for tissue and bone applications

Hyoung Seop Kim

Department of Materials Science and Engineering, POSTECH, Pohang, Korea (hskim@postech.ac.kr)

Since the time of Aristotle, through recent history beginning in the late Renaissance, biomechanics field owes its progress to the pioneering work of engineers and scientists starting in the 1960s and 1970s, a period that saw the application of rigorous engineering analyses to the study of biological tissues.
Recently, one of the most pressing needs is to characterize the mechanical properties of various bones and tissues in relation to their micro and macro structures, to better understand their function. However, it was widely known that the elementary engineering analyses, and that would normally suffice to describe conventional engineering materials, were generally inadequate for modeling biological tissues and bones.
In bone mechanics, though bone behaved as a linear elastic material to within a reasonable approximation, it was found to be anisotropic, exhibiting properties that varied consistently with the spatial orientation of its microstructure. Many soft tissues were similarly observed to be anisotropic, often undergoing large deformations during normal function, and to exhibit significant viscoelasticity.
In this presentation, the finite element method based on continuum constitutive models such as crushable and viscous models was employed in order to investigate the mechanical properties of tissues and bones. Model materials were used for targeting materials. In particular, fracture and densification behavior in bones under compressive loads and deep indenting behavior in tissues were simulated.

[1] Fung, 1981 Y.C. Fung, Biomechanics: Mechanical Properties of Living Tissues **Vol. xii**, Springer, New York (1981) 433 pp.

Mechanical properties of TiO_2 coating by ECR plasma oxidation

Makoto Fujikawa[1,4], Yusuke Orii[1,4], Hiroshi Masumoto[2], Takashi Goto[3], Yoshitomo Honda[4], Takahisa Anada[4], Keiichi Sasaki[1], Osamu Suzuki[4]

[1] *Division of Advanced Prosthetic Dentistry, Tohoku University Graduate School of Dentistry, Sendai, Japan,* [2] *Center for Interdisciplinary Research, Tohoku University, Sendai,* [3] *Institute for Materials Research, Tohoku University, Sendai, Japan ,* [4] *Division of Craniofacial Function Engineering, Tohoku University Graduate School of Dentistry, Sendai, Japan*
fujikawa-thk@umin.ac.jp

The difference in thermal expansion of Ti and TiO_2 film is relatively large, which is one of the reasons of the difficulty in preparing the desirable TiO_2 film on Ti at low temperature for a short time. On the other hand, Electron cyclotron resonance (ECR) plasma is high-active plasma and suitable for generating highly quality crystalline films at low temperatures. The surface characteristics determined to change the parameters of substrate temperature, oxidation time and total pressure. The surface conditions control the induction of calcium phosphate, octacalcium phosphate ($Ca_8H_2(PO_4)_6 \bullet 5H_2O$; OCP), nucleation and the growth. OCP has been suggested to be a precursor of initial mineral crystals in biological apatite in bone, dentin, and enamel. Previous studies indicated that OCP facilitates osteoblastic cell differentiation in vitro and bone regeneration in various bone defects. Thus, OCP should be one of candidates to improve osteoconductive property of the metallic implant. However, mechanical properties of TiO_2 film itself by ECR plasma oxidation are not reported.

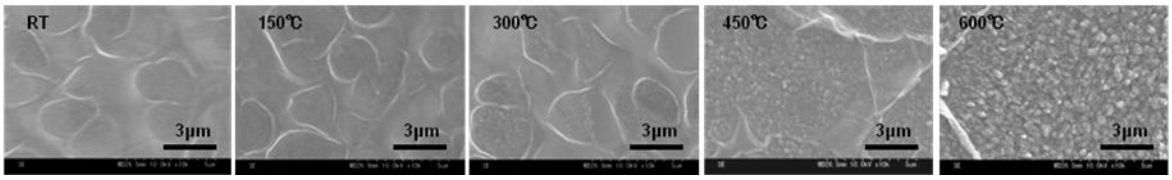

Micrographs of the surfaces of TiO_2 films
(ECR conditions fixed 0.015Pa and 30min, to change substrate temperature)

We examined the good condition of heating substrate temperature by ECR plasma oxidation, that is around 300°C. The adhesion strength became maximum value at 613 kg/cm^2. Adhesion strength increased with increasing substrate temperature less than 300°C. And the strength, more than 300°C, decreased with increasing substrate temperature. From the results of adhesion strength, it is guessed that the surface micrograph of TiO_2 showed a crater-like smooth surface of around 3μm is good surface property. On the other hand, it is thought that the surface micrograph, many small particle-shaped grains around 0.5μm into the rough and large crater-like surface the size more than 10μm, is not so good. And more, the figures related to the result of

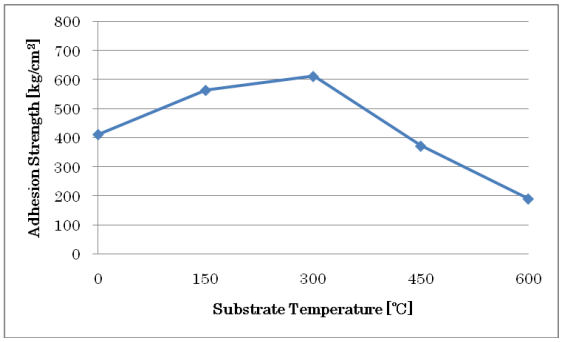

ECR conditions fixed 0.015Pa and 30min,
to change substrate temperature

roughness of the TiO_2 film. It was suggested that the roughness increased with increasing substrate temperature. And thickness increased with higher temperature to oxidize by ECR plasma.

It is possessed that the highest adhesion strength, approximately 613 kg/cm^2 with 0.015Pa, 300°C, 30min, has enough resistance for detachment of implantation in human body. Furthermore the strong adhesion is provided in the condition that it is easy to comparatively operate. Therefore, ECR plasma oxidation is effective method of surface modification of Ti substrate.

The Dynamic Deformation Response of a High-Strength, High-Toughness 10Ni-0.1C Steel

R. Gupta, P. Wang* and K.S. Kumar
Division of Engineering, Brown University, Providence, RI 02912
* Currently at UES, Inc, Dayton, OH 44135

We have characterized the propensity for adiabatic shear band formation under dynamic deformation conditions in an ultra-high strength (1.1GPa) 10Ni steel and demonstrated that in spite of its outstanding static toughness, this steel is highly prone to shear localization and failure. Specifically, microstructural evolution during deformation of a Fe-10 Ni-0.1C-Cr,Mo,V steel was examined. In the high-strength condition, the steel has a lath martensite microstructure with a mean lath size of ~60 nm, and MC carbides dispersed in it with a mean size of ~20 nm. During compressive dynamic deformation using a split Hopkinson bar (strain rates of 1000 to 4000 per second), depending on strain and strain rate, shear localization occurs and is accompanied by an optically visible shear band (~20 micrometers wide). In the situation where the localization process is in its early stages (lower rates, lower global height strains, or both), the microstructure shows severe local deformation within the band but the initial microstructure is still discernible. With progression in severity of localization, there is clear and reproducible evidence for a central region (~6-8 micrometers wide) within the shear band composed of ~300 nm size equiaxed grains. Electron microscopy characterization of these grains by extracting specimens from the shear band using a FIB confirms the presence of both, austenite, with a low dislocation content, and heavily dislocated and/or twinned ferrite. Composition measurements from the individual grains using EDX in the TEM confirm partitionless transformation. The fine grain size and the high Ni content in this alloy together are thought to stabilize the austenite phase in the band and prevent its reversion to martensite, thereby enabling confirmation of a phase transformation within the band. When the test conditions are further intensified, a crack "chases" the shear band, with the crack running either partway or all the way through the band and therefore through the sample. Examination of the resulting fracture surfaces provides significant evidence for the presence of a thin liquid film layer (perhaps 10-20 nm or less) with no shear resistance that led to fracture. Together, these observations provide a microstructural footprint for how deformation progresses during shear localization, and a sense for the accompanying thermal profile within the shear band.

.

Evaluation of different surface modifications for implant alloys in vivo

Yuko Suzuki, Takashi Goto*, Masahiro Yoshimura*,**, Rong Tu*, Masatoshi Takahashi, Toshie Kuwana, Osamu Suzuki and Keiichi Sasaki

Graduate School of Dentistry, Tohoku University

**Institute for Material Research, Tohoku University*

***Materials and Structures Laboratory, Tokyo Institute of Technology*

osuzu-thk@umin.ac.jp

Introduction

Titanium (Ti) and its alloys have been widely used for dental and orthopedic implants because of their excellent biocompatibility. Hydroxyapatite (HAp) coating on implant alloy is one of the methods used to improve their osseointegration. In the present study, the bone bonding strength and histology were examined about two different films formed by Radiofrequency (RF) magnetron sputtering and Growing Integration Layer (GIL) method on cpTi and Bulk Metallic Glasses (BMG).

Materials and Methods

Commercially pure Ti (cpTi) and BMG were used in this study. The specimens were cylinder shape (Φ3*10 mm) . Amorphous HAp film with a thickness of 200 nm was fabricated on cpTi and BMG samples using an RF magnetron sputtering system with HAp targets and GIL film was formed on BMG by hydrothermal- electrochemical method. The specimens were implanted into the tibiae of eighteen male Japanese white rabbits weighing about 3 kg. The experimental groups were as follows (eight animals in each group); cpTi as control (cpTi), cpTi with HA film (HApTi), BMG with HAp film (HApBMG), BMG with GIL film (GILBMG). At 4 and 8 weeks after the implantation, animals were sacrificed and the push-out test was performed. After the push-out test, the implant surfaces were observed by scanning electron microscopy (SEM). The tibiae were embedded in methylmethacrylate (MMA) resin and were sectioned for histological analysis.

Results and Discussion

The bone-implant shear strength in the HApTi group at 4 weeks was significantly higher than that in the cpTi group, but decreased until 8 weeks and approached that of the cpTi. On the other hand, there was no difference between HApBMG and GILBMG. The finding in this study suggests that BMG had few advantages for osseointegration, but the HAp film formed by RF magnetron sputtering was effective for bone-implant fixation in early stage.

Influence of immediate and early loading on bone metabolic activity around dental implants in rat tibia

M. Yamamoto*[1], M. Yokoyama[1], S. Koyama[2], Y. Funaki[3], Y. Kikuchi[5], K. Nakamura[5], K. Nakazawa[5], H. Yamazaki[4], K. Ishii[4,5], K. Sasaki[1]

Division of Advanced Prosthetic Dentistry, Tohoku University Graduate School of Dentistry[1], Maxillofacial Prosthetics Clinic, Tohoku University Hospital, Sendai, Japan[2], Division of Radiopharmaceutical Chemistry, Tohoku University Cyclotron Radioisotope Center[3], Division of Radiation Protection and Safety Control, Tohoku University Cyclotron Radioisotope Center[4], Division of Quantum Science and Energy Engineering, Tohoku University Graduate School of Engineering[5]

【Introduction】The prosthetic treatment for missing teeth by dental implants has been proven to be a predictable and successful treatment procedure. In these days, various loading protocols have been developed because of increased demand for shorten treatment period and less complicated surgery. Although a lot of studies about immediate and early loaded implants have been reported, few biological evidences to support these concepts are available. Moreover there is no study of longitudinal examination by using nuclear medicine approach. This study aimed to examine the influence of immediate and early loading on dynamic changes of bone metabolism around dental implants by using a newly developed high resolution PET scanner.

【Materials and Methods】Two titanium implants (φ 1.2 mm) were inserted parallel to each other in the tibiae of wistar rats (12 weeks) and perpendicular to the bone surface with the superior portion of the implant exposed. 1 day after insertion, closed coil springs with 4.0 N were applied to the expose superior portion of the implant for 4 weeks to apply a continuous mechanical stress. The rats with $^{18}F^-$ (5 mCi/rat) intravenously-injected were scanned by a high resolution PET scanner at 4, 7, 14, 28 days after load application. Round ROI (region of interest)s were defined around the implants (right tibia) and the same area at the intact side (left tibia). Accumulation counts of $^{18}F^-$ at each ROI were examined. Then, longitudinal dynamic changes in bone metabolism around titanium implants were evaluated.

【Results and Conclusion】Bone metabolic activity initially increased until 7 days. Afterwards, they gradually decreased from the peak level to the pre-loading level despite a static force being applied to the implants. These results, which are consistent with our previous report (JOMI 2008), suggested this change may be attributed to an adaptive bone remodeling process. Further investigation is needed to examine the influences of different timings of loading on metabolic activity around dental implants.

Evaluation of calcium phosphate coating film fabricated by RF magnetron sputtering on titanium substrate

K. Ueda[1], T. Narushima[1], Y. Kawasaki[1], T. Goto[2], J. Kurihara[3], H. Kawamura[3]
[1)]*Department of Materials Processing, Tohoku University*
[2)]*Institute for Materials Research, Tohoku University*
[3)]*Department of Dentistry, Tohoku University*

1. Introduction

Titanium and its alloys have been widely used as implant materials in many applications because of their excellent mechanical properties, high corrosion resistance and biocompatibility. Calcium phosphate is the main inorganic component of bone and has excellent biocompatibility with bone. Since titanium implants are required strong and rapid fixation to bone, the calcium phosphate coating on titanium is one of the most useful techniques to improve the biocompatibility with bone. RF magnetron sputtering is one of the methods to coat bioactive ceramic films under low processing temperature condition.

In this study, the interface between the titanium substrate and calcium phosphate coating film fabricated using RF magnetron sputtering was investigated. TEM observation and bonding strength measurements were conducted for the as-deposited coating films, and the coated titanium implants were implanted into the femur of rabbits.

2. Experimental procedures

Amorphous calcium phosphate (ACP) and oxyapatite ($Ca_{10}(PO_4)_6O$, OAp) coating films with a thickness of 0.5 μm were fabricated using RF magnetron sputtering on the mirror-polished and blast-treated titanium substrates. Interfacial observation of the as-deposited coating film was carried out using TEM. The bonding strength between the coating film and substrate was evaluated using a mechanical strength tester. ACP coating film was fabricated on the surface of the blast-treated screw-type titanium implants and they were implanted into the femur of Japanese white rabbits and the removal torque was evaluated. SEM observation of the cross section of the blast-treated screw-type titanium implants after removal torque measurements was conducted.

3. Results and discussion

Figure 1 shows the TEM images of the interface between mirror-polished titanium substrates and ACP and OAp coating films. The uniform and dense film contacted to titanium substrate directly and firmly. The bonding strengths between the coating films and the titanium substrates were greater than 60 MPa, and the values were independent of the phase of the coating films and surface roughness of the substrates. The removal torque of the ACP-coated screw-type titanium implants from the femur of rabbits after 2-week implantation was higher than that of the non-coated one.

The ACP coating film was not observed at the interface between blast-treated titanium implants and the bone after 4-week implantation by the SEM. It was speculated that the ACP coating film would be dissolved because of its high bioresorbability. On the other hand, the crystalline calcium phosphate coating films remained at the interface.

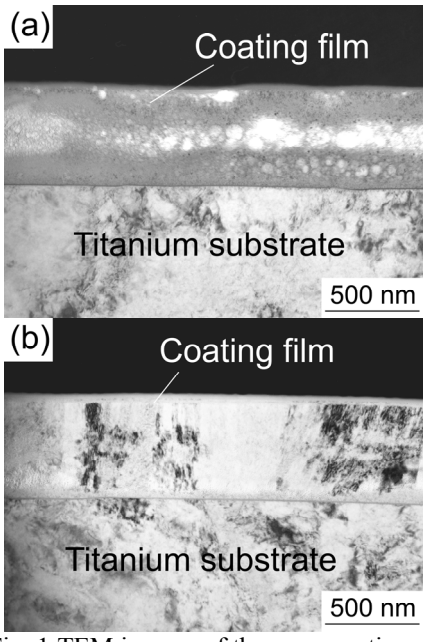

Fig. 1 TEM images of the cross section of the (a) ACP and (b) coating films fabricated on the mirror-polished titanium substrates.

Surface modification of pure titanium and cell-materials interactions

Z.X. Chen, Y. Takao, W.X. Wang, T. Matsubara and L.M. Ren
Research Institute for Applied Mechanics, Kyushu University
zxchen@riam.kyushu-u.ac.jp

Titanium is frequently used for orthopedic and dental implants for its excellent mechanical properties, chemical stability and biocompatibility. Its biocompatibility is closely related to the properties of the surface layer, in terms of its morphology, structure and composition. Therefore, various surface modification techniques have been developed and applied to titanium implants in an attempt to obtain the most biocompatible surface. Among these techniques, anodization methods have attracted great attention because the surface TiO_2 layer fabricated by anodization not only can show various surface morphologies, but also contain valuable chemical species incorporated from the electrolyte. Furthermore, anodization methods can adapt to any shaped titanium implants and easily be applied in industrial practice.

In this work, the surface of pure titanium was modified by anodization treatment in phosphoric acid solution since phosphate ions enriched surface oxide layers can promote cell attachment/growth. Anodization was carried out in potentiostatic mode at different voltages: 100V, 200V and 300V. Surface characteristics of obtained anodic TiO_2 layers and their influence on the cell response were investigated. Micrographs by scanning electron microscopy revealed that the dense and uniform oxide layer obtained at 100V exhibits a nanostructured surface which is similar to the surface of natural tooth cementum. In contrast, porous oxide layers without nanometer features were produced at higher voltages. Thin film X-ray diffraction analysis confirmed the existence of anatase in the oxide layer obtained at 300V, but not in oxide layers obtained at 100V and 200V. In vitro cell-materials interactions study demonstrated greater cell adhesion and proliferation on the oxide layer obtained at 100V compared to other two kinds of oxide layers.

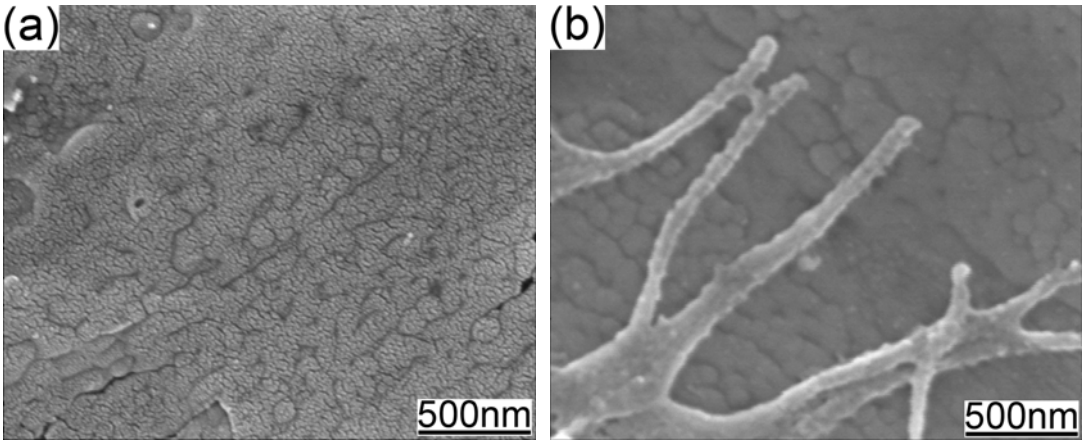

SEM micrographs showing (a) nanostructured surface of the oxide layer obtained at 100V and (b) cell adhesion on the nanostructured surface.

Intracellular signal transduction during mechano-response in differentiating chondrocytes

Ichiro Takahashi[1], Taisuke Masuda[2], Kumiko Kohsaka[3], Fumie Terao[3], Takahisa Anada[2], Yasuyuki Sasano[4], Teruko Takano-Yamamoto[3], Osamu Suzuki[2]

[1]*Section of Orthodontics, Kyushu University Faculty of Dental Science,*
takahashi@dent.kyushu-u.ac.jp
[2]*Division of Craniofacial Function Engineering,*
[3]*Division of Orthodontics and Dentofacial Orthopedics,*
[4]*Division of Craniofacial Development and Regeneration,*
Tohoku University Graduate School of Dentistry

Differentiation of mesenchymal cells and metabolism of skeletal tissues have been considered to be regulated by multiple factors, such as growth factors, cytokines, interaction between extracellular matrices and mechanical stress. Bone and cartilage are the supportive tissue for body action consisted of tissue specific extracellular matrices (ECMs) and specifically differentiated cells, osteocyte and chondrocytes, in each tissue. Cartilages contribute to bone growth under the mechanical compressive stress and to buffering the mechanical stress in joint action. Thus, the mechanical stress could be one of the important regulatory factors, which affects to the differentiation of chondrocytes from mesenchymal stem cells. Here, we are presenting the intracellular signal transduction through extracellular signal-regukated kinase (ERK) pathway during the inhibition of chondrocyte differentiation from mesenchymal stem cells by mechanical tensile stimulation.

To investigate the roles of ERK-1/2 on mechano-response of differentiation of chondrocyte, in vitro analysis was performed using mesenchymal stem cells derived from embryonic limb bud of rats. Micromass culture on a custom made multi-axial two-dimensional mechanical stress loading cell culture system (Fig. 1) was developed to evaluate the effect of stepwise mechanical stretch on chondrogenic differentiation of mesenchymal stem cells, and to assay the phosphorylation and gene expression of ERK-1/2. In addition, to evaluate the role of ERK-1/2, the activation of ERKs was inhibited by U0126 and PD98059. These experiments indicated that chondrogenesis was inhibited by mechanical stretch. By loading tension force, ERK-1/2 was activated directly, while gene expression was not affected. Inhibiting this activation of ERK signaling pathway, chondrogenesis was rescued to normal level from tension-mediated inhibition.

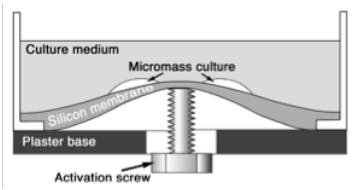

Fig. 1 Custom-made stepwise stretch culture system

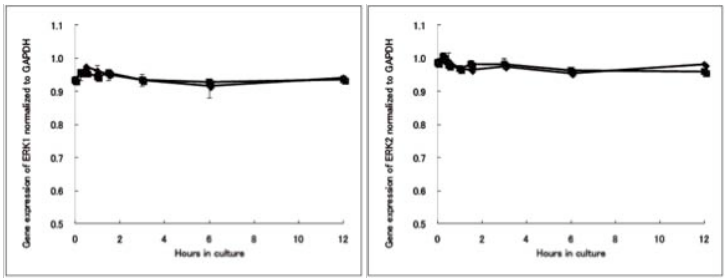

Fig. 2 Gene expression of ERK-1/2 during stretch stimulation evaluated by semi-quantitative PCR

Thus, mechanical stretch induced activation of ERK-1/2 signaling pathway can be considered as one of the key regulatory mechanism in chondrogenesis.

Biodegradation behaviors of Mg exposed in vitro and in vivo surroundings

Hyun Kwang Seok, Korea Institute of Science and Technology(KIST), Korea
(+82-2-958-6738, drstone@kist.re.kr)

Mg(and its alloys) is considered as candidate material for biodegradable orthopedic implant, vascular stent, bone graft, and scaffold because of its ease corrosion in body fluid, reasonable mechanical properties and excellent bio compatibility. However, it is somewhat difficult to control both bio degradation rate and mechanical strength simultaneously because very limited degree of freedom in selecting alloying element is allowed in order not to sacrifice bio compatibility.

In this presentation, most of the time would be devoted to explain “how we could successfully control the biodegradation rate of pure Mg by controlling impurity contents, and both mechanical strength and degradation rate of Mg alloys by controlling the contents of additional elements such as Ca, Zn, Mn”. Also, the effect of materials process such as extrusion and heat treatment on the variation of mechanical and chemical properties of Mg and its alloys will be briefly discussed. In additions, some activities for fundamental research about cell behavior and metallurgical phenomena by implantation of Mg into alive animal will be introduced.

Synergetic Effect of Sandblasted and Acid-Etched Surface and Statin on Peri-implant Osteogenesis.

Yasuko Moriyama, Yasunori Ayukawa, Ikiru Atsuta, Yohei Jinno,
Tomohiro Masuzaki, Kiyoshi Koyano
Division of Oral Rehabilitation, Faculty of Dental Science,
Kyushu University, Fukuoka, Japan
kabay@dent.kyushu-u.ac.jp

Objectives: It has been indicated that a sandblasted and acid-etched (SA) implant had a grater bone-implant contact. On the other hand, it has been demonstrated that HMG-CoA reductase inhibitors ("statins"), which are widely used for cholesterol lowering, stimulates bone formation. We previously showed that local application of fluvastatin at the implant site enhanced the osteogenesis around the titanium implant in early stages of healing. The aim of the present study was to investigate the effects of SA surface on peri-implant osteogenesis under the influence of statin, using a rat model.

Methods: Titanium implants were inserted in both tibiae of 10-week-old Wistar rats. Experimental groups included: (1) control (machined surface implant); (2) SA (sandblasted and acid-etched implant); (3) FS (machined surface implant with 75μg fluvastatin-containing PGA (used as a carrier)); (4) SA ＋ FS (SA implant with 75μg fluvastatin-containing PGA). The animals were sacrificed on 1, 2 and 4 weeks of observation. Peri-implant bone formation was assessed using histomorphometric procedures by measuring both bone-implant contact (BIC) and the volume of the newly formed peri-implant bone (BV). Removal torque value (RTV) was also performed to evaluate the shear strength between bone and implant. Statistical differences among groups were determined by ANOVA and $P<0.05$ was considered significant.

Results: At week 1, BIC, BV and RTV were significantly higher in SA + FS group than those in other groups. BIC was significantly increased in FS group compare to control group and SA group. RTV was significantly higher in SA group and FS group than those in control group. At week 2, there was no significant difference in BIC values among the groups, however, BV was significantly increased in FS group in comparison with other groups. RTV denoted the similar tendency with BV at 2 weeks. At 4 weeks, there were no significant differences among the groups.

Conclusion: Our histomorphometrical and mechanical evaluations revealed the synergetic effect of SA surface and statin on peri-implant osteogenesis.

Characterization of microstructure and mechanical properties of biodegradable PLLA polymer blends with LTI

Vilay Vannaladsaysy[1,2], M. Todo[1],M. Mariatti[2], Zulkifli Ahmad[2]
[1] *Research Institute for Applied Mechanics, Kyushu University, Kasuga, Fukuoka, Japan*
[2] *School of Materials & Mineral Resources Engineering, Universiti Sains Malaysia, 14300 Nibong Tebal, Pulau Pinang, Malaysia*
[3] *Department of Mechanical Engineering, National University of Laos, Vientiane, Laos*
villayv@gmail.com

Poly(L-lactic acid) (PLLA) is gaining attention in the medical field for application areas such as sutures, antibiotic release, and macroscopic temporary implants. PLLA bioresorbable implants have advantages in repair and generation of healing tissues, providing biodegradability, biocompatibility with proper mechanical performance. However, PLLA exhibits brittle fracture behavior and therefore, the toughening of PLLA becomes one of the most important issues in the field of bio-polymer engineering. Blending with a ductile biodegradable polymer such as poly (ε-caprolactone) (PCL) is known to be an effective way. It is however also known that in general such PLLA/PCL blend exhibits phase-separation morphology.

In the present study, PLLA and PCL pellets were blended using a conventional melt-mixer. The blend ratios of PCL were chosen to be from 10 to 75 wt.%. High viscous solution of LTI was also added during blending process. The mixtures were then molded using a hot press, and then followed by cooling process to produce sheets of 2mm thick. SENB specimens were then prepared from the sheets. PLLA/PCL and PLLA/PCL/LTI with 50wt.% PCL are denoted thereafter as AL_{50} and ALI_{50}, respectively.

The morphology of the blends was investigated by observing cryo-fractured surfaces of the specimens using FE-SEM to characterize the microstructural modification. FT-IR measurement was carried out to analyze the chemical structures of the blends. The mode I fracture tests of the SENB specimens were also performed to evaluate the mode I fracture energy, J_{in}, at crack initiation. The fractured surfaces of the SENB specimens were also observed by FE-SEM to characterize the fracture micromechanism and the effect of LTI addition on the fracture behavior.

As typical examples, the cryo-fractured surfaces of AL_{50} and ALI_{50} are shown in Fig.1. A phase separation is clearly observed on AL_{50}, and the dispersed phase is thought to be PLLA. On the contrary, ACI_{30} with LTI does not exhibit such dispersed phase, indicating that the immiscibility between PLLA and PCL was dramatically improved by LTI addition.

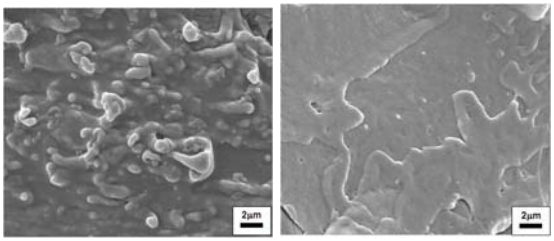

(a) AL_{50} (b) ALI_{50}

Fig.1 FE-SEM micrographs of cryo-fractured surfaces.

Fig. 2 shows the FT-IR spectra patterns. It is seen that PLLA, PCL and the blends exhibited very similar spectra patterns with the C=O peak at about 1700 cm^{-1}. It is clearly seen that the C=O peak of ALI_{50} became lower than that of AL_{50}, suggesting that the mobilities of PLLA and PCL molecules were reduced due to LTI addition. On the other hand, the spectra of LTI was obviously characterized by the existence of the large NCO peak around 2200 cm^{-1}. It is noted that there was no apparent peak of NCO in the spectra of ACI_{20}, indicating that NCO

groups were chemically reacted with OH groups existing at the ends of PLLA and PCL molecules. It is thus concluded from these FT-IR results that LTI works as a compatibilizer connecting between PLLA and PCL molecules.

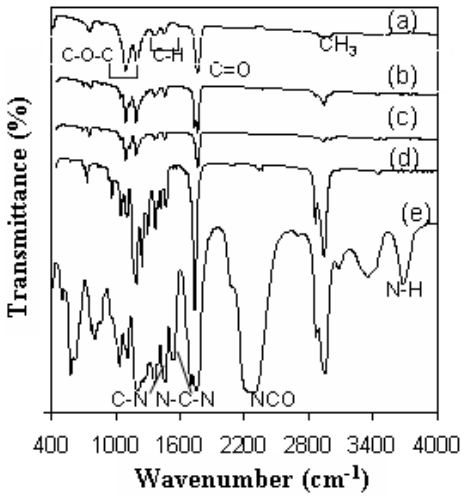

Fig. 2. FT-IR spectra: (a) PLLA, (b) AL_{50}, (c) ALI_{50}, (d) PCL and (e) LTI.

The initial fracture energy, J_{in}, is shown in Fig.3. It is seen that J_{in} of AL blends were slightly higher than that of neat PLLA, indicating the effectiveness of blending; on the contrary, J_{in} of ALI increased with increase of PCL content, these experimental results clearly exhibited that LTI addition effectively improved the mode I fracture property.

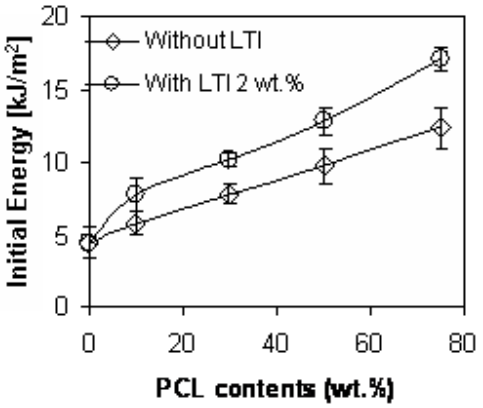

Fig. 3 Initial fracture energy as a function of PCL content.

FE-SEM micrographs of fracture surfaces in the crack initiation regions are shown in Fig.4. It is noted that these fracture surfaces of PLLA/PCL blends are much rougher than that of neat PLLA that exhibits very smooth surface, corresponding to the higher energy dissipation on the fracture surfaces of the blends than that of PLLA. It is apparent that the elongation of the fibril structures in AL blends seems to be larger than that in ALI blends. Many voids are also observed on the AL surfaces; on the other hand, such voids do not exist on the ALI surfaces. Thus, this kind of voids are thought to be formed as the traces of removed PCL or PLLA spherulites. Such voids cause localized stress concentrations in the surrounding regions, resulting in acceleration of fracture initiation. Therefore, the fracture initiation in ALI blends without any voids is much slower than that in AL blends. It is concluded that this kind of delay of fracture initiation results in the improved fracture energy shown in Fig.3.

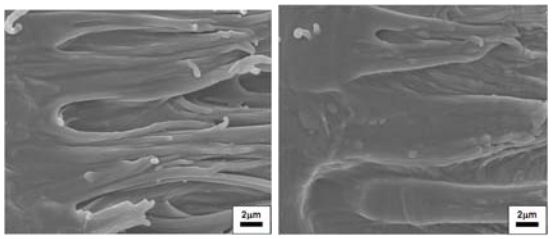

(a) AL_{50} (b) ALI_{50}

Fig. 4 FE-SEM micrographs of mode I fracture surfaces.

In summary, it was found that LIT addition dramatically improves the immiscibility between PLLA and PCL due to chemical reaction between NCO and OH groups, resulting in the effective improvement of the mode I fracture energy of PLLA/PCL polymer blends.

Acknowledgement: This work was funded by AUN/SEED-Net and JICA is gratefully acknowledged. The authors greatly acknowledge the support from Kyushu University and Universiti Sains Malaysia.

Comparative studies of the peri-implant epithelium of rat gingivae between “Step-type” and “Straight-type” implant system

Atsuta I, Ayukawa Y, Ogino Y, Moriyama Y, Jinno Y, Koyano K

Section of Removable Prosthodontics, Division of Oral Rehabilitation

Faculty of Dental Science Kyushu University

atyuta@dent.kyushu-u.ac.jp

Purpose

The “platform-switched” implant system has emerged as one of the effective implant treatment. However, supportive basic studies in this system have not yet been reported. To prove the importance of this system, we have evaluated the attachment of peri-implant epithelium (PIE) to the implant surface, comparing the “Step-type” and “Straight-type” implant model, respectively.

Methods

Six-week-old male Wistar rats were used for the “Step-type” and “Straight-type” implant experimental model. The experiments are as follows; (1) the down-growth of PIE is investigated in the long term, (2) the comparison of penetration of Horseradish peroxidase (HRP) as an exogenous factor, laid on the gingival margin around the implant body, with four models.

Results and Conclusion

(1) The down-growth of PIE: The “Step-type” implant system could not block the PIE elongating apically. These results in two models have no significant differences. However, the “Step-type” can protect down-growth rather than “Straight-type” in the long term, (2) The penetration of an exogenous factor: “Step-type” can inhibit penetration of HRP from the gingival sulcus into the connective tissue under the PIE, compared with “Straight-type”. These findings suggest that this system is effective for the sealing of the epithelium-implant interface.

References

Hermann F, Lerner H, Palti A. Factors influencing the preservation of the periimplant marginal bone. Implant Dent. 16:165-75, 2007.

Atsuta I, Yamaza T, Yoshinari M et al. Ultrastructural localization of laminin-5 (gamma2 chain) in the rat peri-implant oral mucosa around a titanium-dental implant by immuno-electron microscopy. Biomaterials. 26: 6280-7, 2005.

Temporal changes in the ultrastructural localization of bone proteins at the bone-titanium interface of rat

Yasunori Ayukawa, Kiyoshi Koyano
Division of Oral Rehabilitation, Faculty of Dental Science,
Kyushu University, Fukuoka, Japan

<Purpose> The purpose of this study was to investigate both temporal and spatial changes in the distribution of bone proteins, types I and III collagen (ICol, IIICol), osteocalcin (Ocl) and osteopontin (Opn), at the early stage of bone healing around the titanium (Ti) implant in rat tibiae.
<Methods> The implant was placed in rat tibiae and at 7, 14 and 28 days post-implantation, animals were sacrificed and specimens were embedded into acrylic resin. Ultrathin sections were made and immunostaining was performed using post-embedding immunogold procedure, to determine which bone proteins were present at the interface, and observed with transmission electron microscopy.
<Results> An electrondense 20-50-nm thick amorphous layer was interposed between the bone and the Ti. In addition, in the sections of both 7 and 14 days, fine fibrous layer was intervened between the amorphous layer and the bone. On the immuno-transmission electron microscopic observation, the labelings for both Ocl and Opn were widely distributed on the newly formed bone, but especially accumulated in the fibrous layer and in electron-dense patches in the bone. An amorphous layer was labeled with both Ocl and Opn. In addition, although fine fibrous layer was labeled strongly with Opn, Ocl and IIICol, labeling for ICol was absent.
<Conclusion> The amorphous layer contained both Ocl and Opn. Both proteins may play an important role in the cell adhesion onto the Ti surface.ICol-free fibrous layer was seen in the initial stage of bone healing around the implant. It suggests that this layer may be later remodeled into normal ICol-rich bone because such layer was not observed at 28days. In addition, since ICol is the only collagen which can be a mineralized bone matrix, bone mineralization was initiated from the outer side of periimplant bone and the closest area to the implant was not mineralized at an early stage of bone healing.
The purpose of this study was to investigate the distribution of osteocalcin (Ocl) and osteopontin (Opn) around hydroxyapatite (HA) implants in rat tibiae during the early stage of bone healing. Implants were placed in rat tibiae. Seven days post-implantation, the animals were sacrificed, and tissue specimens were fixed, demineralized, dehydrated, and embedded in acrylic resin. Each implant was removed, using the fracture technique, and then re-embedded in the same resin. Semi-thin survey sections, 1-μm thick, were stained with toluidine blue and

observed with light microscopy. Ultra-thin sections were also made, immunostained using a post-embedding immunogold procedure, and observed with transmission electron microscopy, to determine which bone proteins were present at the interface. In the 1-μm semi-thin sections, the bone appeared to be in direct contact with the HA, except where cells, thought to be osteoblasts, were seen on the HA. However, the transmission electron microscopic observations showed an electron-dense amorphous layer, 20-50 nm thick, interposed between the bone and the HA. Sometimes, a fine fibrous layer was also seen, between the amorphous layer and the bone. The interposed cells appeared to be osteoblasts, and were seen on the HA; however, they directed their basolateral surface toward the HA. The immuno-transmission electron microscopic observations showed widely distributed labeling for both Ocl and Opn on the newly formed bone. Furthermore, labeling for both proteins was accumulated in electron-dense patches in the bone and at the osteocytic lacunae. The amorphous layer interposed between the titanium and the bone was labeled strongly with Ocl, but weakly with Opn. The fibrous layer located between the amorphous layer and the bone was labeled strongly with both Opn and Ocl. The orientation of the interposed cells suggests that they did not secrete the bone matrix directly onto the HA surface. The protein-rich fibrous layer seen around the implant in the initial stage of bone healing may later be remodeled into normal type I collagen-rich bone, as this layer has not been mentioned in reports dealing with bone histology around HA in the late healing stage. The large amounts of Ocl and small amounts of Opn in the amorphous layer suggest that these proteins may regulate mineralization close to the HA, and may also mediate cell-matrix, cell-HA, and matrix-HA adhesion along the HA.

References :

Ayukawa Y, Takeshita F, Inoue T, Yoshinari M, Shimono M, Suetsugu T, Tanaka T. An immunoelectron microscopic localization of noncollagenous bone proteins (osteocalcin and osteopontin) at the bone-titanium interface. J Biomed Mater Res 1998;41:111-119.

Ayukawa Y, Takeshita F, Inoue T, Yoshinari M, Ohtsuka Y, Murai K, Shimono M, Suetsugu T, Tanaka T.
An Ultrastructural study of the bone-titanium interface using pure titanium-coated plastic and pure titanium rod implants. Acta Histochem Cytochem 1996;29:243-254.

This study was partially supported by a Grant-in-Aid for Scientific Research(B), No. 10480246, from the Ministry of Education, Science and Culture of Japan.

Corrosion behavior of the Japanese cup-yoke-type magnetic attachments

Yukyo Takada, Masatoshi Takahasi and Masafumi Kikuchi
Tohoku University Graduate School of Dentistry
takada@mail.tains.tohoku.ac.jp

Cup-yoke-type dental magnetic attachments are composed of a magnetic assembly and a keeper fixed in the denture and the root caps, respectively. Attractive force between the magnetic assemblies and the keepers retains a denture in the oral cavity. In this study, corrosion behavior of the Japanese cup-yoke-type magnetic assemblies was electrochemically evaluated by anodic polarization curves in 0.9% NaCl solution at 310K.

The magnetic assemblies such as Magfit DX800 (Aichi Steel), Gigauss D800 (GC), Hyper Slim 4013 and Hicorex Slim 4013 (Hitachi Metals) were used for the anodic polarization curve, and ferritic (444, XM27 and 447J1) and austenitic (316L) stainless steels composing the magnetic assemblies were also examined as controls. Distribution of elements in the laser welding zones between the yokes and the shield ring was analyzed using EPMA.

Anodic polarization curves showed that all magnetic assemblies broke down in the range of 0.6-1.1V (Fig.1). After the magnetic assemblies were subjected to anodic polarization from the rest potential to 1.5 V, their corrosion areas clearly revealed that the weld zone on the shield ring of any magnetic assembly had corroded (Fig. 2). However, any breakdown potentials were significantly higher ($p < 0.05$) than that of 316L used for the shield rings (Fig.1).

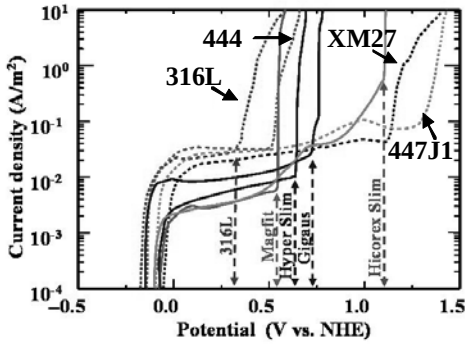

Fig.1 Anodic polarization curves of the magnets and stainless steels (0.9%NaCl solution at 37°C)

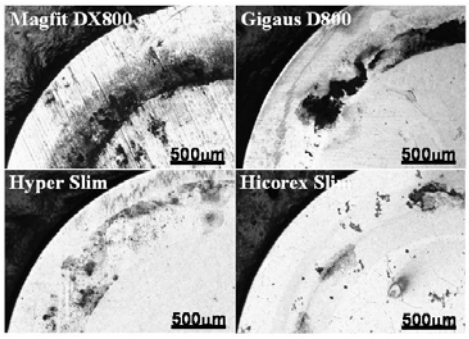

Fig.2 Surface conditions of the magnets after anodic polarization to 1.5 V (0.9%NaCl solution at 37°C)

EPMA showed that, except in Magfit DX800, the Cr contents of the weld beads on the shield rings were larger than those of 316L. The laser welding resulted in an increase in the breakdown potentials of the magnetic assemblies.

These magnetic assemblies are expected to maintain good corrosion resistance in the oral cavity because they show breakdown potentials sufficiently higher than that of 316L.

Effect of amino acids on Zn-release from Zn-containing OCP

Yoshitomo Honda[1], Takahisa Anada[1], Hiroyuki Kubota[2], Akio Harada[2], and Osamu Suzuki[1]*

1 Tohoku University Graduate school of Dentistry, Craniofacial Function Engineering,

2 Tohoku University School of Dentistry

honda-y@mail.tains.tohoku.ac.jp, anada@m.tains.tohoku.ac.jp

**suzuki-o@mail.tains.tohoku.ac.jp*

Introduction

Zinc-containing calcium phosphates (Zn-CaPs) are attractive materials to treat bone resorption induced by osseous diseases, such as osteoporosis. Zn ion has a marked potential to promote bone formation and suppress bone resorption, while serious side effects are possibly caused when used at an excess dose. Therefore, controlling the Zn-release from the Zn-CaP is required for the safe and effective usage of Zn-CaP. Elucidation of the mechanisms is indispensable for developing a novel Zn-CaP. Up to now, several Zn release mechanisms have been proposed. However, little attention has been given to the amino acids which are ubiquitously distributed in body fluid and tissues. The purpose of this study was to investigate the effect of amino acids on Zn-release from two Zn-CaPs, Zn-containing octacalcium phosphate and hydroxyapatite (Zn-OCP and Zn-HA) which have different solubility. Zn-OCP was newly developed in order to reveal the association between Zn-release cased by the amino acid and the conventional Zn-release depending on the dissolution of the Zn-CaP.

Materials and methods

Zn-OCPs containing various contents of Zn were synthesized by a modified wet synthesis method reported previously [1]. Zn-HAs were prepared by hydrolysis of Zn-OCP slurries in the hot water at 70˚C. In order to evaluate the dissolution rate and the Zn-released-behavior of Zn-OCPs and Zn-HAs in the various solutions, changes of calcium (Ca) and Zn concentrations were determined by means of the colorimetrical methods using commercially available Ca-E test Wako and Zn-test Wako kits. Two types of the solutions were prepared as solvent: (1) 0.1 M HEPES buffer (pH=7.4) with/without various concentrations of amino acids, (2) alpha modified eagle minimum essential medium (α-MEM). Zn-CaPs were immersed in these solvents, and the supernatants were utilized for the quantification of the Ca and Zn concentration. Solid/solution ratio of the slurries was settled to the 1 g/L at all examinations. Concentrations of the amino acids in the 0.1 M HEPES buffers referred to that of alpha-MEM (L-Lysine HCl: 73 mg/L, L-Cysteine HCl･H_2O: 100 mg/L, L-Histidine HCl･H_2O: 42mg/L, L-Aspartic acid: 30 mg/L, L-Glutamic acid: 75 mg/L).

Results and discussion

Dissolution of Zn-OCP was similar to original OCP. Among the 5 selected amino acids, cysteine and histidine induced effectively Zn-release from the both Zn-CaPs. Given the common property of these amino acids, Zn chelating reaction is supposed to be associated with Zn release from the Zn-CaP.

From the comparative study of both Zn-CaPs, Zn-release caused by the amino acid was not completely correlated with the dissolution tendency.

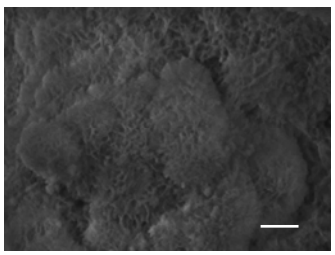

SEM image of the Zn-OCP. Bar=2 μm

Conclusion

It has been reported that the systemic amino acid concentrations were changed by ages and systemic diseases. Present finding suggests that the local concentration of amino acid should be considered for the use of Zn-CaP. Additionally, regulation of amino acids around the Zn-CaPs is supposed to be a new target for fabricating the safe and effective Zn releasing CaP.

Reference

1: O. Suzuki *et al.*: Tohoku. J. Exp. Med., 164 (1991) 37.

Development of Artificial Bone Substitute Composed of Bioactive MegaGen Synthetic Bone and Osteoconductive Hyaluronic Acid Hydrogels

Sei Kwang Hahn,[1,*] Junseok Yeom,[1] Jung Ho Je,[1] Dong Jun Yang,[2] Hong-In Shin [3]

[1] *Department of Materials Science and Engineering, POSTECH, Korea*

[2] *MegaGen Co. Research Institute of Science and Technology, Korea*

[3] *Department of Oral Pathology, School of Dentistry, Kyungpook National University, Korea*

A novel artificial bone substitute composed of bioactive MegaGen Synthetic Bone (MGSB) and hyaluronic acid (HA) hydrogels was successfully developed for bone tissue engineering applications. HA is known to play important roles in bone regeneration due to its angiogenic and osteoconductive characteristics. Accordingly, HA hydrogel was designed to supply HA continuously for effective bone regeneration by its controlled degradation *in vivo*. Four kinds of HA hydrogels were synthesized with different degradation kinetics in the range of 1~6 months in the body: adipic acid dihydrazide modified HA (HA-ADH) hydrogels, HA hydrogels crosslinked with divinyl sulfone (DVS), cystamine (CYS), and gelatin (GEL), respectively. MGSB composed of hydroxyapatite (60 wt%) and β-tricalcium phosphate (β-TCP, 40 wt%) was prepared by the chemical precipitation method. Seven different samples of a control, Bio-OSS®, MGSB, Bio-OSS®/HA-ADH hydrogels, MGSB/HA-DVS hydrogels, MGSB/HA-CYS hydrogels, and MGSB/HA-GEL hydrogels were implanted to the calvarial critical size bone defects of New Zealand white rabbits. Histological and histomorphometric analyses revealed that MGSB/HA-GEL hydrogels resulted in the most effective bone regeneration compared to other samples. The bone regeneration by MGSB/HA-GEL hydrogels in 8 weeks was as high as 55% occupying 75% of the bone defect area with MGSB in the form of a calvarial bone plate. The bone regeneration was also analyzed by synchrotron X-ray imaging, which clearly visualized 3-dimensional micron scale morphologies of regenerated bones being interconnected with the bone substitute. The novel artificial bone substitute will be investigated further for clinical applications with X-ray imaging study to visualize the bone regeneration process.

Tailoring mechanical properties of PLLA-based scaffolds by structural control

Joo-Eon Park and Mitsugu Todo
Research Institute for Applied Mechanics, Kyushu University
park@riam.kyushu-u.ac.jp

Many research works have been conducted to develop porous structure materials in the field of tissue engineering because such porous biomaterials, so-called scaffold, are very important in regenerative medicine in order to culture stem cells to form target tissue or organ. In general, bioabsorbable materials such as bioactive ceramics and biogedradable polymers are considered to be used for scaffolds. When a scaffold is implanted into the damaged tissue in human body, it must have suitable mechanical properties compatible to the mechanical properties of the tissue. The mechanical properties such as elastic modulus and strength of scaffold can be controlled by changing the composition, the porosity and the other structural futures.

In this research, novel porous scaffolds with reinforced structures were developed by using a typical biodegradable polymer, poly(L-lactide) (PLLA) and the solid-liquid phase separation and the freeze dry methods. One of the newly developed scaffold is the beam reinforced type in which one to four beams are embedded into the scaffold as load bearing structures. The other scaffold is the layered type in which solid outer layer is surrounding porous inner structure.

SEM micrograph of micro-structure of the one beam reinforced scaffold is shown in Fig.1. This reinforced scaffold exhibits a homogeneous pore distribution in outer layer, and the pore morphology becomes smaller towards the central beam. It is thought that the outer side-surface of the beam reinforcement is dissolved by the 1, 4Dioxane when beam is placed in PLLA-Dioxane solution in PP tube, therefore, the concentration of the surrounding solution near the beam surface is increased.

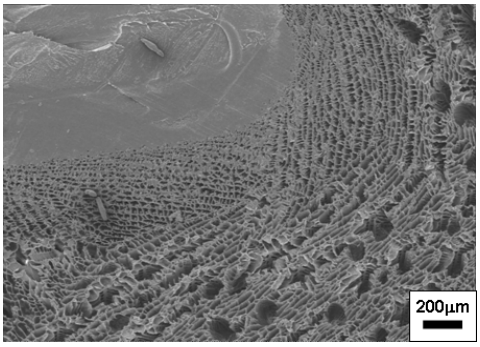

Fig.1 Micro-structure of beam reinforced scaffold.

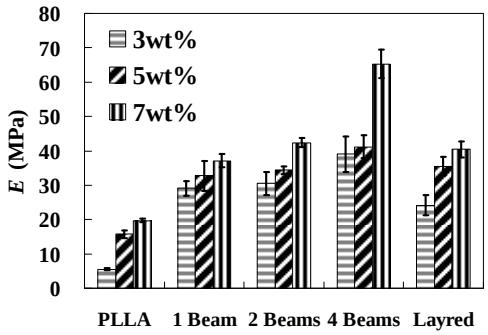

Fig.2 Effects of concentration and reinforced structures on compressive modulus.

Effects of solution concentration and reinforced structures on the compressive elastic modulus of scaffolds are shown in Fig.2. It is clearly seen that the modulus effectively increases by reinforcements. It is also found that the modulus of the 2-beam scaffold is about the same as that of the layered scaffold. It is also noted that the compressive strength effectively improved by the reinforcements. Cell adhesion behavior on the surfaces of these scaffolds was also found to be good.

Biomechanical risk assessment for fully edentulous maxilla with dental implants

Takaaki Arahira[1], Mitsugu Todo[2], Yasuyuki Matsushita[3], Kiyoshi Koyano[3]
[1]*Graduate School, Kyushu University, Kasuga, Fukuoka*
[2]*RIAM, Kyushu University*
[3]*Faculty of Dental Science, Kyushu University*
arahira@riam.kyushu-u.ac.jp

Occlusion function of the patients with fully or partially edentulous jaw bones can effectively recovered by implant treatment. Although implant technology is advancing and the safety and durability of implants are improving, some biomechanical problems such as implant fracture and bone resorption around implants still exist and have been one of the most important issues needed to be solved in dental science. For fully edentulous jaw bones, optimization of implant treatment including determination of the number, length, position and angle of implants is performed by dentists only without biomechanical consideration, therefore, success of implant treatment for a patient strongly depends on the ability and experience of the dentist. If the biomechanical conditions of jaw bones after implant treatment are understood prior to the treatment, such information is greatly helpful for the dentist to conduct the treatment successfully and result in reduction of clinical problems.

In the present study, computational analysis of a fully edentulous maxilla with implants was performed in order to assess effects of the number and position of embedded implants on the stress state of the maxilla. The maxilla model was constructed from CT data of an elderly patient and for simplicity, a part of maxilla was modeled as shown in Fig.1. 3, 4 and 6 implants were embedded in the maxilla independently and a prosthesis was attached to the tops of the implants. It should be noted that in the actual clinical treatment for this patient, 4 implants were chosen as the decision made by the dentist. The boundary condition is shown in Fig.2. The top of the maxilla model was totally fixed, and the distributed load was applied to the surface of the prosthesis. As an example of the analytical results, the maximum strain energy density in the vicinity of the molar implant is shown in Fig.3. The strain energy density value in the 3-implant model was much higher than those of the 4- and 6-implant models. It is noted that the energy value of the 4-implant model was close to that of the 6-implant model, suggesting the safety of the 4-impant treatment.

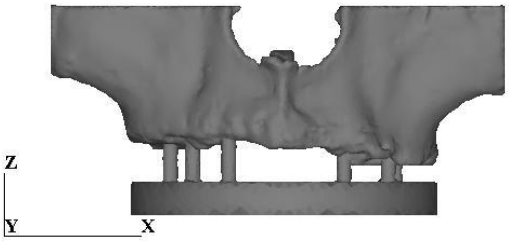

Fig.1 Maxilla model with implants

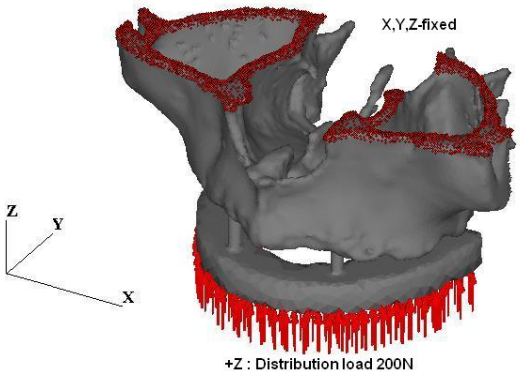

Fig.2 Boundary condition.

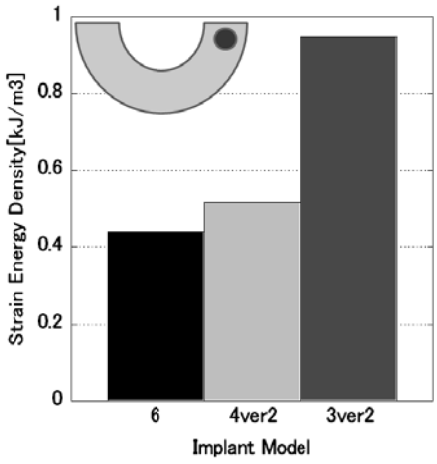

Fig.3 Maximum strain energy density.

Detection of microorganisms from inside of acrylic resin prostheses

Yasuhisa Takeuchi [1, 2], Kazuko Nakajo [2], Takuichi Sato [2], Yoko Sakuma [1, 2], Shigeto Koyama [3], Keiichi Sasaki [1] and Nobuhiro Takahashi [2]

[1, 2] Division of Advanced Prosthetic Dentistry, and [2] Division of Oral Ecology and Biochemistry, Tohoku University Graduate School of Dentistry, Sendai, Japan

[3] Tohoku University Hospital, Dental Center, Sendai, Japan.

Introduction

Acrylic resin is one of the major materials for dental prostheses because of its physicality and moldability suitable for dental prostheses. It is well known that using acrylic resin dental prostheses in the oral cavity for a long term, oral microorganisms adhere to the surface of dental prostheses and probably invade into the acrylic resin. Following proliferation of microorganisms within acrylic resin dental prostheses, these microorganisms are thought to relate with the oral and respiratory infectious diseases.

Many researchers have reported on the microorganisms that adhere to the surface of acrylic resin dental prostheses. However, there is little information on the microorganisms within acrylic resin dental prostheses. In Zao conference, August, 2007, we showed the existence of viable bacteria within acrylic resin denture bases and isolated 4 bacterial genera, *Lactobacillus*, *Actinomyces*, *Propionibacterium* and *Streptococcus* sp.

In the present study, we aimed to detect the microorganisms from the acrylic resin obturator of dent-maxillary prosthesis, which is one type of the dental prostheses for post-maxillectomy patients. In addition, the results were compared with our previous findings of acrylic resin denture base.

Materials and Methods

Ten dent-maxillary prostheses-attached closed hollow obturators were collected from ten patients. Informed consent was obtained from each patient. After disinfecting the denture surface with 70% ethanol, the wall of obturator was pierced with a sterile round bur. Inner fluid was collected with a sterile syringe. In the absence of inner fluid, 1.0 mL of 40 mM potassium phosphate buffer (pH 7.0) was alternatively injected to the obturator and collected. Ten-fold dilutions of these fluids were inoculated onto blood agar plates and incubated under aerobic and anaerobic conditions at 37°C for 7 days. After the incubation, all colonies from plates were sub-cultured and identified by 16S rRNA gene sequence analysis.

Results

Bacteria were detected from 7 out of 10 samples. Thirteen bacterial genera were identified from obturators of dent-maxillary prostheses, and *Bacillus*, *Klebsiella*, *Lactobacillus* and *Propionibacterium* sp. were predominant.

Conclusion

It was revealed that viable bacteria existed in closed hollow obturators of dent-maxillary prostheses. The predominance of *Lactobacillus* and *Propionibacterium* sp. was similar to our previous results of microbial profile detected within acrylic resin denture bases, suggesting the acrylic resin provides a suitable environment to these oral bacteria. The additional detection of opportunistic bacteria, *Bacillus* and *Klebsiella* sp., was unique and suggests a diverse environment in the obturators of dent-maxillary prostheses.

Porous alginates scaffolds containing various amount of octacalcium phosphate crystals

Naru Shiraishi [1, 2,] Takahisa Anada [1,] Yoshitomo Honda [1,] Taisuke Masuda [1,] Keiichi Sasaki [2,] Osamu Suzuki [1,*]

[1] *Division of Craniofacial Function Engineering (CFE), Tohoku Univ.,*

[2] *Division of Advanced Prosthetic Dentistry, Tohoku Univ.*

** Osamu Suzuki [suzuki-o@m.tains.tohoku.ac.jp]*

Introduction: Octacalcium phosphate (OCP; $Ca_8H_2(PO_4)_6 \cdot 5H_2O$) has been proposed to be a precursor of apatite crystals in bone and tooth. Synthetic OCP has a potential to facilitate bone regeneration in comparsion with hydroxyapatite (HA; $Ca_{10}(PO_4)_6(OH)_2$) due to its stimulatory capacity in osteoblastic differentiation[1),2)]. We previously prepared three-dimensional alginate(Alg)/OCP scaffold by co-precipitation method[3)]. We reported that increasing pore size of the scaffolds improves cell attachment in vitro and bone regeneration in vivo. In this study, we designed to investigate whether the amount of OCP affects the characteristics of Alg/OCP scaffolds fabricated by simple mixing method.

Materials and Methods: Four % alginate solution and OCP powders were mixed and homogenized. The mixture was crosslinked with Ca^{2+} by adding 50 mM calcium chloride solution. To eliminate the excess Ca^{2+} ions, the slurries were centrifuged and the supernatant was removed. The slurries were re-suspended in water. The slurries containing different amount of OCP (w/w % = 100/0, 75/25, 50/50, and 25/75) were prepared. These slurries were lyophilized to form porous scaffolds. The Alg/OCP composites were characterized by X-ray diffraction (XRD), fourier transform infrared spectroscopy (FTIR), and scanning electron microcopy (SEM). The porosity and pore size were quantified by mercury intrusion porosimetry. The uniaxial compressive test was carried out. The scaffolds were immersed in simulated body fluid (SBF) for up to 14 days, and then lyophilized for FTIR spectroscopy and SEM observation.

Results and Discussion: There was no change in XRD and FTIR characteristic peaks of crystal structure of OCP before and after mixing with Alg. SEM observation revealed that OCP crystals were homogeneously dispersed in the Alg matrix. The pore size and elastic modulus increased depending on the amount of OCP. After immersed in SBF, FTIR spectra showed that characteristic peaks of OCP became obscured with time, and acicular morphology of OCP crystals became noclear under SEM observation. The results suggested that OCP in the scaffolds can be converted into HA in SBF. In conclusion, the present Alg/OCP scaffolds prepared by simple mixing method have the potential providing a better scaffold for cell proliferation and enhancement of bone regeneration.

[1)] O. Suzuki et al., Biomater. (2006), [2)] T. Anada et al., Tissue Eng. (2008), [3)] Fuji T et al., Tissue Eng Part A. (2009) in press.

Mechanical performances of biomedical Ti and Zr system alloys through thermomechanical treatments

Toshikazu Akahori*, Mitsuo Niinomi*, Masaaki Nakai*, Harumi Tsutsumi*,
Tomokazu Hattori** and Hisao Fukui***
*Departiment of Biomaterials Science, Institute for Materials Research,
Tohoku University
**Department of Materials Science and Engineering, Meijo University
***School of Dentistry, Aichi-Gakuin University
akahori@imr.tohoku.ac.jp

Titanium (Ti) and its alloys, in particular, alpha + beta-type Ti alloys such as Ti-6Al-4V ELI and Ti-6Al-7Nb alloys have been used as biocompatible metallic materials. Their Young's moduli are, however, still higher comparing with that of the cortical. A new beta-type Ti alloy composed of non-toxic and allergy-free elements like Nb, Ta, and Zr, Ti-29Nb-13Ta-4.6Zr alloy (TNTZ) proposed by present authors, has been developed in order to achieve relatively low Young's modulus and excellent mechanical performance. On the other hand, zirconium (Zr) has been also paid attention as metallic biomaterial for the next generation because of good biocompatibility nearly equal to or a few GPa smaller Young's modulus as compared to Ti alloys showing low Young's modulus. In this study, mechanical performances such as tensile and fatigue characteristics, and biocompatibility of biomedical TNTZ with low Young's modulus subjected to thermo-mechanical treatments, and Zr-Nb system alloys were investigated in order to judge their potential for biomedical applications.

Young's modulus of as-solutionized TNTZ ($TNTZ_{ST}$), which was around 63 GPa, was pretty similar to that of as-cold-rolled TNTZ ($TNTZ_{CR}$). The Young's moduli of commercially pure Ti (CP Ti) and hot-rolled Ti-6Al-4V ELI alloy (Ti64) were respectively around 110 GPa. The Young's moduli of $TNTZ_{ST}$ and $TNTZ_{CR}$ were approximately a half of CP Ti and Ti64, and are approximately twice as large as that of the cortical bone. Tensile properties of $TNTZ_{ST}$, $TNTZ_{CR}$ and $TNTZ_{CR}$ subjected to high pressure torsion (HPT), which is one of severe deformation processes, at rotations of 1, 5 and 10 are shown in **Fig. 1**. The tensile strength of $TNTZ_{CR}$ subjected to HPT increase remarkably according to the number of rotation. The tensile strength is in particular over 1000 MPa at a rotation of 5 or more. In this case, the tensile strength of $TNTZ_{CR}$ subjected to HPT at a rotation of 5 is 1.4 and 2.3 times larger than those of $TNTZ_{CR}$ and $TNTZ_{ST}$, respectively, while the elongation shows the reverse trend. From these results, it is possilbe to control the tensile strength and elongation of TNTZ with single β phase, which are more than 1000 MPa and around 10%, respectively.

Zr-XNb system alloy (X: 0-30mass%) showed the smallest value of Young's modulus (around 58 GPa) at Nb content of 20mass%. In the case of implantation of the bars made of Zr-XNb system alloys into the lateral femoral condyle of mature Japanese rabbits, the tendency of contact between the cancellous bone and the bar became remarkably at 24 weeks after the implantation according to increasing Nb content.

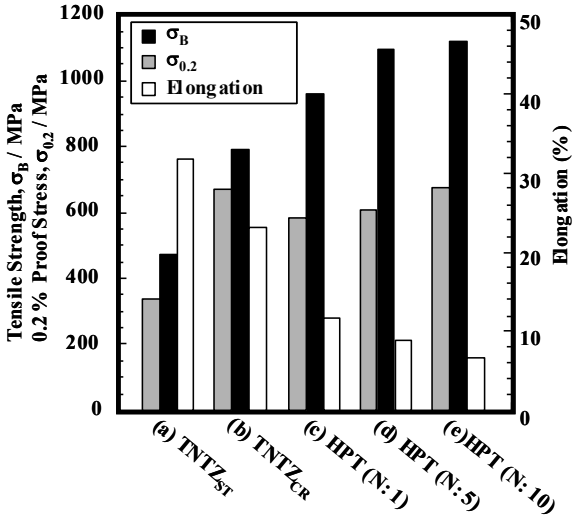

Fig. 1 Tensile properties of (a) $TNTZ_{ST}$, (b) $TNTZ_{CR}$ and $TNTZ_{CR}$ subjected to (c) HPT(N: 1), (d) HPT (N: 5) and (e) HPT (N: 10).

Dynamic globularization behavior and bio-mechanical compatibility of Ti-13Nb-13Zr alloy

Chan Hee Park, Young Soo Chun and Chong Soo Lee*

Department of Materials Science and Engineering,
Pohang University of Science and Technology (POSTECH), Pohang 790-784, Korea

Abstract

This study aims to achieve enhanced mechanical compatibility of Ti-13Nb-13Zr alloy by producing submicrocrystalline microstructure without imposing severe strains. In order to find the optimum processing conditions, a series of compression tests was performed for initial martensite microstructure in the strain range of 0.8-1.4, the strain rate range of 10^{-3}-1 s^{-1} and the temperature range of 500-700 ^{o}C. Based on the microstructure analysis, the submicrocrystalline (~0.4 μm) alloy having over 80 % of high-angle grain boundaries was produced via dynamic globularization at temperature of 600 ^{o}C, equivalent strain rate of 10^{-1} s^{-1} and strain of 1.4, which showed much enhanced mechanical compatibility as compared to the conventionally produced ones. The formation of submicrocrystalline microstructure at relatively low strain was rationalized by examining the microstructure before and after dynamic globularization.

*Corresponding author and presenter
Prof. Chong Soo Lee:
Tel.: +82 54 279 2141, Fax: +82 54 279 2399. E-mail: cslee@postech.ac.kr

Improvement in mechanical properties of spinal implant rod made of Ti-29Nb-13Ta-4.6Zr

Kengo Narita[1, 3], Mitsuo Niinomi[2], Masaaki Nakai[2], Toshikazu Akahori[2], Harumi Tsutsumi[2], and Kazuya Oribe[3]

[1]*Graduate Student, Tohoku University, Sendai, Japan*
[2]*Institute for Materials Research, Tohoku University, Sendai, Japan*
[3]*Showa Ika Kogyo. Co., Ltd, Toyohashi, Japan*

Implanting a spinal fusion using metallic implant rods is one of the effective treatments for spinal diseases. Ti and Ti alloys are mainly used in abovementioned implant rods. They must have high fatigue strength in order to prevent failure of implant rod in human body. Recently, not only high fatigue strength but also low Young's modulus equal to that of cortical bone is simultaneously required in order to inhibit bone absorption. Ti-29Nb-13Ta-4.6Zr (mass%) alloy (referred to as TNTZ) has been developed as a metallic biomaterial. TNTZ is composed of only non-toxic elements. Additionally, Young's modulus of TNTZ exhibits lower than that of conventional implant rod made of Ti-6Al-4V ELI. Thus, TNTZ is highly expected to be applied to the implant rod practically. However, with regard to the four-point bending fatigue strength, no advantage was shown in TNTZ in comparison with Ti-6Al-4V ELI alloy (Ti64) previously. Therefore, improvement in mechanical properties of TNTZ rod by optimizing thermo-mechanical treatment was investigated in this study.

A hot-forged bar made of TNTZ was subjected to solution treatment or cold swaging (ST-Rod$_{as}$ or SW-rod$_{as}$). Subsequently, they were subjected to aging treatment at 673 K or 723 K for 259.2 ks (ST-Rod$_{673K}$ and ST-Rod$_{723K}$ or SW-Rod$_{673K}$ and SW-Rod$_{723K}$, respectively). Their microstructures were evaluated by optical microscopy, transmission electron microscopy, and X-ray diffraction analysis. Further, their mechanical properties were evaluated through tensile test and Young's modulus measurement with free resonance method.

The results of tensile test are shown in Fig.1. While the elongation is lower, the tensile strength of ST-Rod$_{723K}$ is higher than that of ST-Rod$_{as}$ because of the α phase precipitation. While the decrease in elongation is large, the tensile strength of ST-Rod$_{673K}$ is increased more greatly than that of ST-Rod$_{723K}$ by the α and ω phase precipitations. The tensile properties of TNTZ rod are drastically improved by cold swaging before aging treatment; the tensile strength of SW-rod$_{673K}$ and SW-rod$_{723K}$ are about 300-350MPa higher, but its elongation is comparable to that of ST-rod$_{673K}$ and ST-rod$_{723K}$, respectively. SW-rod$_{723K}$ shows a good balance between tensile strength and elongation. The tensile strength of SW-rod$_{723K}$ is 200MPa higher than that of Ti64 rod. Further, the elongation of SW-Rod$_{723K}$ is similar to that of Ti64 rod. Therefore, fatigue properties of SW-rod$_{723K}$ are expected to have advantage to that of Ti64 rod.

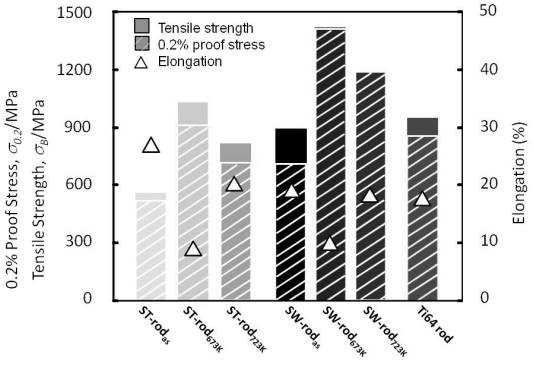

Fig. 1, Tensile properties of Ti-29Nb-13Ta-4.6Zr subjected to solution treatment(ST-rod$_{as}$), cold swaging (SW-rod$_{as}$),and aging treatment at 673 K or 723 K for 259.2 ks after solution treatment or cold swaging(ST-rod$_{673K}$, ST-rod$_{723K}$, SW-rod$_{673K}$, and SW-rod$_{723K}$, respectively) and Ti64 rod.

Precipitates formed in biomedical Co-Cr-Mo alloys with various carbon contents

S. Mineta[1], Alfirano[1], S. Namba[2], T. Yoneda[3], K. Ueda[1], and T. Narushima[1]
[1]*Department of Materials Processing, Tohoku University, Sendai, Japan.*
[2]*Materials Research Laboratory, Kobe Steel, Ltd., Kobe, Japan.*
[3]*Yoneda Advanced Casting Co., Ltd., Takaoka, Japan.*
e-mail: a9td5609@cs.he.tohoku.ac.jp

1. Introduction

Co-Cr-Mo alloys have been widely used as metallic biomaterials because of their high mechanical strength, corrosion resistance and wear resistance. These properties are generally associated with the phase, size, shape and distribution of carbides in the microstructure. Many manufacturers currently subject Co-Cr-Mo alloys to heat treatments such as solution treatment or aging in order to remove cast defects and improve their mechanical properties. Therefore, the behavior of precipitation or dissolution of carbides is essential knowledge for establishing the reasonable processing of Co-Cr-Mo alloys with low cost. The objective of this study is to investigate the microstructural change in Co-Cr-Mo alloys with various carbon contents during solution treatment and aging.

2. Experimental procedures

Four carbon level ingots used in this study were prepared by vacuum furnace melting; their chemical composition was Co-28Cr-6Mo-xC (x = 0.12, 0.15, 0.25, and 0.35mass%). The specimen alloys are hereafter referred to as C12, C15, C25 and C35. The as-cast alloys were solution treated at 1473 to 1548 K for 1.8 - 43.2 ks, followed by water quenching. The aging behavior of these alloys was investigated after solution treatment at 1523 K for 43.2 ks. Aging temperature was varied from 873 to 1473 K. The maximum holding time in aging was 44.1 ks. Microstructural observation was carried out using OM and SEM. Precipitates were electrolytically extracted from the alloys using 10%H_2SO_4 aqueous solution and then characterized using XRD and observed using SEM.

3. Results and discussion

A dendrite matrix and interdendritic and grain boundary precipitates were observed in the as-cast alloys. Figure 1 shows XRD patterns of the

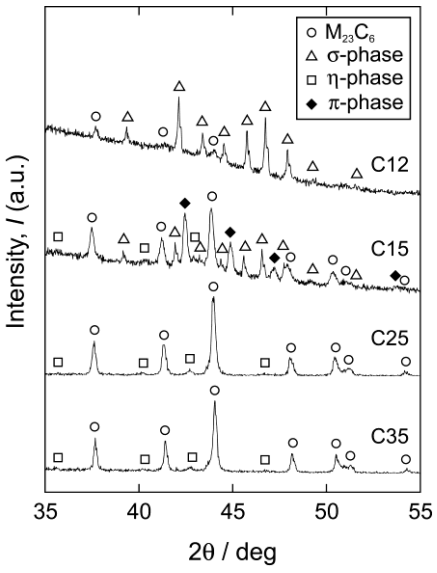

Fig. 1 XRD patterns of precipitates electrolytically extracted from as-cast C12, C15, C25, and C35 alloys.

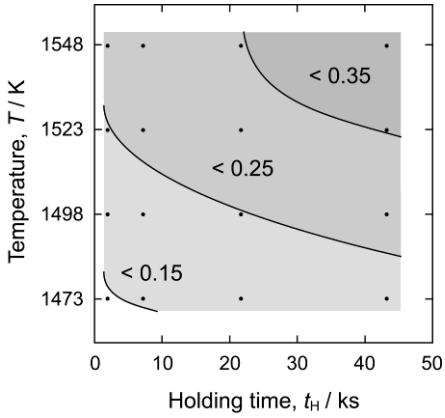

Fig. 2 Solution treatment conditions for the complete dissolution of precipitates in Co-Cr-Mo alloys

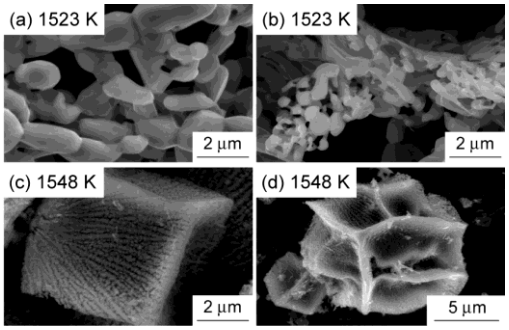

Fig. 3 SEM images of precipitates electrolytically extracted from as-cast C35 alloys solution treated at 1523 K in (a) and (b), and 1548 K in (c) and (d) for 1.8 ks.

precipitates electrolytically extracted from the as-cast C12, C15, C25, and C35 alloys. The phase of the precipitates in the alloys depended on the carbon content. The precipitates observed in the matrix of the C12 alloy, a low carbon level alloy, were an $M_{23}C_6$ type carbide and an intermetallic σ-phase. In the C25 and C35 alloys, high carbon levels alloys, an $M_{23}C_6$ type carbide, and η-phase (M_6C-$M_{12}C$ type carbide) were detected. In the case of C15 alloy, the pattern was complicated and revealed the presence of another phase in addition to the $M_{23}C_6$ type carbide, a σ-phase, and a η-phase. This phase was deduced to be M_2T_3X type carbide with a β-manganese structure (π-phase).

Complete precipitate dissolution was observed in all four carbon level alloys, and solution treatment conditions for complete precipitate dissolution in Co-Cr-Mo-C alloys are shown in Fig.2. It was clarified that the holding time required for complete precipitate dissolution increased with increasing carbon content and decreased with increasing solution treatment temperature. The $M_{23}C_6$ type carbide with dense and porous morphology were detected during the solution treatment at 1473, 1498, and 1523 K, while at 1548 K, the carbide had cubic or star-like shape with stripe patterns (Fig. 3).

C12, C25, and C35 alloys were solution treated at 1523 K for 43.2 ks in order to dissolve precipitate completely and then they were subjected to the aging experiments. The Time-Temperature-Precipitation diagram of these alloys could be constructed (Fig. 4). In C25 and C35 alloys, the precipitation was detected in the wide region of aging temperature and holding time as compared with that in C12 alloy. Precipitated carbide was $M_{23}C_6$ type in C25 alloy, and the size of the carbide increased with increasing aging temperature and holding time.

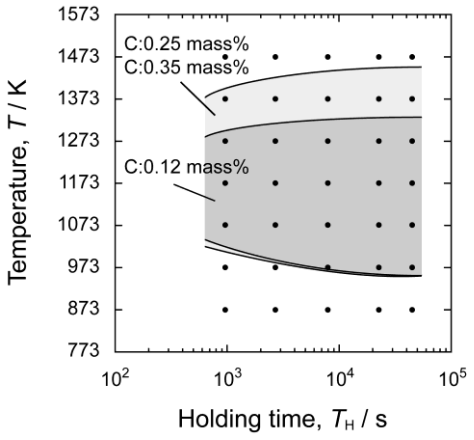

Fig. 4 Time-Temperature-Precipitation (TTP) diagram in Co-Cr-Mo alloys.

Thermomechanical Characterization of Bulk Metallic Glasses

Kwang Seok Lee

Korea Institute of Materials Science, Materials Processing Division, Materials Deformation Group, 531 Changwondaero, Changwon 641-831, South Korea

Abstract

Since bulk metallic glasses (BMGs) are naturally metastable phase compared to their crystalline counterpart, BMGs have the possibility of unintended crystallization during isothermal annealing or warm deformation for considerable time within supercooled liquid region (SLR), which introduces (nano)crystallization-induced embrittlement; for this reason it is highly desirable in avoiding crystallization during any processing within SLR to maintain the extraordinary rheological properties of BMGs in their amorphous state. In this regard, high temperature deformation behavior and formability of Zr- and CuZr-based bulk metallic glasses (BMGs), what I carried out for last several years, will be presented as follows in detail:

1. High temperature deformation behavior of Zr- and CuZr-based bulk metallic glasses
2. Formability evaluation of both Monolithic and Multiphase Zr-based bulk metallic glasses
3. Influence of the warm process condition on the structural change and macroscopic post-processed feature of bulk metallic glasses

Preparation and Bioactivation of Zr-Al-Co Bulk Metallic Glasses

Takeshi Wada[1], Fenxiang Qin[1], Xinming Wang[1], Akihisa Inoue[1],
Naota Sugiyama[2], Rieko Ito[2], Nobuhiro Matsushita[2]

[1]*Institute for Materials Research, Tohoku University, Sendai, Japan*
[2]*Materials and Structures Laboratory, Tokyo Institute of Technology, Yokohama, Japan*

Bulk metallic glasses (BMGs) are promising materials for biomedical application because of their superior mechanical and chemical properties compared to conventional crystalline alloys. Especially, Zr-based BMGs are considered to be useful for orthopaedic application because they have high glass-forming ability, good corrosion resistance in biological fluid and low Young's modulus. The Zr-based BMG biomaterials may provide the opportunity to reduce the major concern of the present orthopaedic materials such as bone resorption. For the application of BMGs as orthopaedic fields, it is important of develop Zr-based BMGs with less cytotoxicity and good bioactivity. The Zr-Al-Co system may be useful for this aim because it doesn't contain allergy element of Ni. As shown in the commercial Co28Cr6Mo(wt%) alloys, we can expect good corrosion resistance and less cytotoxicity in this Co containing Zr-based BMGs. Bioactivity (apatite-forming ability) is one important property for orthopaedic materials. The spontaneous formation of hydroxyapatite on the surface of the orthopaedic material enhances the fixation by bonding between human tissue and materials. Recently, the surface bioactivation via low temperature hydrothermal-electrochemical treatment(~393K) in sodium hydroxide solution was reported in Ti-based BMGs. In this presentation, we will report preparation of Zr-Al-Co BMGs. We also investigate the corrosion resistance and cobalt ion release behaviour in simulated body fluid and bioactivation via hydrothermal-electrochemical treatment to examine the possibility of the application of the Zr-Al-Co BMGs as biomedical materials.

Corresponding author: Takeshi Wada (wada-t@imr.tohoku.ac.jp)

Metallic Glass Powders as a binder for poly crystalline diamond

Taek-Soo Kim* and S.M. Shin

[1]*Korea Institute of Industrial Technology, 7-47 Songdo-dong, Incheon 406-840, Korea*

**tskim@kitech.re.kr*

Diamond tools have been widely used in various fields, such as electronics, automotives, construction industries, etc [1]. They are usually prepared by poly crystalline diamond (PCD), cobalt bonded diamond grits as shown in Fig. 1. In order to extend the operating efficiency and life cycle of the tools, a rush of interests are focused to the binding metals exhibiting the advances in wear resistance, corrosion resistance, elastic modulus and strength [2]. It corresponds to the relationship that the weak binder metals controls the whole property of PCD [1].

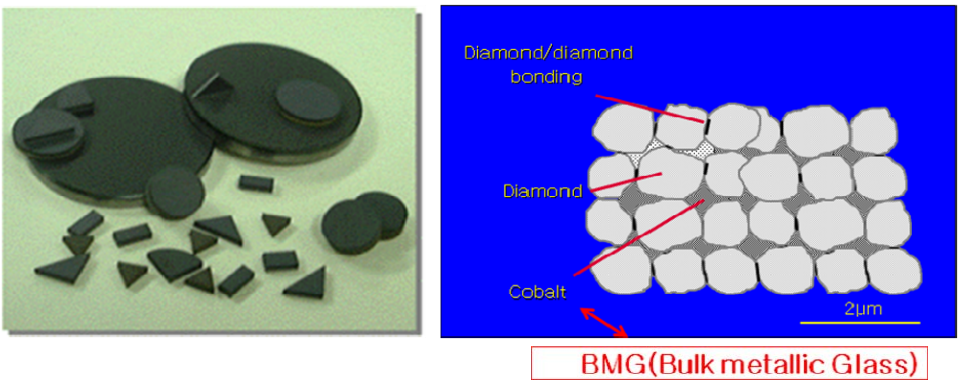

Fig. 1. Shape (left) and schematic (right) of Poly-Crystalline Diamonds (PCD

As an initial step of modifying the metal binders, we tried to replace the conventional binders by the metallic glass (MG) powder as shown in Fig. 1 (Right). The Mg is known to bear an excellent property such as the strength, Young's modulus and corrosion resistance [3].

In the investigation, diamond reinforced Zr based bulk metallic glass matrix composites were fabricated by Spark Plasma Sintering (SPS) process. The effect of diamond size and volume ratio of diamond grits was evaluated on the mechanical properties of composites. Examination of microstructure and evaluation of mechanical properties of the composites were performed depending on the mixing processes. In the condition, WM composite showed the highest mechanical properties. In addition, the experimental results indicated that the mixing method was essential parameters to determine the quality of MG/diamond composites such as the uniformity of phase and binding behavior.

References

[1] J.D.Dwan, Ind. Diam. Rev., 63 (2003) 50.
[2] S.Spriano, Q.Chen, L.Settineri, S.Bugliosi, Wear 259 (2005) 1190.
[3] T.S.Kim, J.K.Lee, H.J.Kim and J.C.Bae, Mat. Sci. Eng. A 402 (2005) 228.

Atomistic interpretation on deformation behavior of bulk metallic glasses

Byeong-Joo Lee

Department of Materials Science and Engineering,
Pohang University of Science and Technology (POSTECH), Pohang 790-784, Rep. of Korea

Abstracts

Understanding the origin of and thus improving the plasticity is one of the hot issues in the bulk metallic glass (BMG) society. Many reports suggest that plasticity of BMGs may be correlated with several properties such as free volume, short range ordered structure, the ratio of shear modulus to bulk modulus, Poisson's ratio, atomic displacement and viscosity. In this study, a special attention was focused on the evaluation of the correlation between the above mentioned properties and plasticity in the Cu-Zr binary BMGs, by comparing the experimentally reported composition dependence with that of various properties obtained from atomistic calculations based on a modified embedded-atom method (MEAM) interatomic potential. It was found that the free volume and the distribution of short range ordered structures have a relatively clear correlation with plasticity. The correlation between the plasticity and other individual properties will also be presented.

Mg-Based Bulk Metallic Glass Composite with Ti Fillers

H. Oka[a]*, H. Kato[b], J. J. Oak[b], K. Yoshimi[c] and A. Inoue[b],

[a] Graduate School of Engineering, Department of Materials Science and Engineering, Tohoku University, Sendai, Japan
[b] Institute for Materials Research, Tohoku University, Sendai, Japan
[c] Graduate School of Environmental Studies, Tohoku University, Japan

(email: *hideki-o@imr.tohoku.ac.jp)

Recently there has been a strong demand of developing a high-strength and high-ductility material with light specific weight for the maintenance of clean atmosphere on the earth through the saving of energy and other natural resources. Among main engineering metallic alloys, Mg metal has advantages of the lowest specific weight, a large amount of deposits on the earth and its easy reuse. Therefore, many efforts have been done for developing new type materials of Mg-based alloys. Mg-based bulk metallic glasses (BMGs) was found to have good castability as well as high compressive strength about 800 MPa which is about four times higher than AZ91 ($Mg_{90}Al_9Zn_1$, a typical high specific strength Mg-based crystalline alloy). However, the Mg-based BMGs do not exhibit appreciable plastic deformation in a uniaxial mode and the improvement on ductility has been strongly requested for the progress in application of Mg-based BMGs. It has been demonstrated that the second phase (i.e., refractory ceramic or metallic particles) dispersed homogeneously in a BMG matrix is effective for improving ductility of BMGs such as Zr-based and Cu-based alloys under a uniaxial compressive mode. In Mg-based alloys, many other types have been developed with ceramic and metallic particles, e.g., TiB_2, ZrO_2, WC, etc. However, there has been no data on the formation of Mg-based BMGMC exhibiting high compressive ductility exceeding 10 %. This paper intends to demonstrate the composite effect of immiscible Ti fillers, powders and fibers to $Mg_{65}Cu_{25}Gd_{10}$ BMG (specific gravity: 3.7 g/cm^3) to improve the ductility of the brittle monolithic Mg-based BMG.

Feasibility of NAPs for the reduction in sintering temperature

Hanshin Choi, Heysook Joo, Chulwoong Han, and Taeksoo Kim
Korea institute of industrial technology, Incheon, Korea

Abstract and keywords

There have been lots of researches to synthesize nano-particles and characterize their unique properties. When it comes to the sintering behavior of nano-particles, sintering temperature can be markedly decreased by reducing particle size owing to the increased surface area and enhanced surface energy. In this study, the effect of particle size on the sintering behavior was used to reduce the sintering temperature. Nano-particle of which chemical composition was same with micro-particles was used as a sintering additive by making nano-attached particle.

Tungsten nano-particles were synthesized by the pulse wire explosion method and then they were blended with micro-particles by wet-blending process. Sintering behavior was evaluated from the relation between sintering temperature and density according to sintering process and feedstock particle. For the micro-sized tungsten particles, denser sintered body at the same thermo-mechanical cycle could be obtained by replacing hot pressing process with spark plasma sintering process. Pulsed current through the particle surfaces in the spark plasma sintering process is well-known to make joule heating and micro-arcing between particles. For the effect of particle feedstock, the addition of nano-particle showed a potential to reduce sintering temperature or make a denser sintered body thank to the size effect on the sinterability.

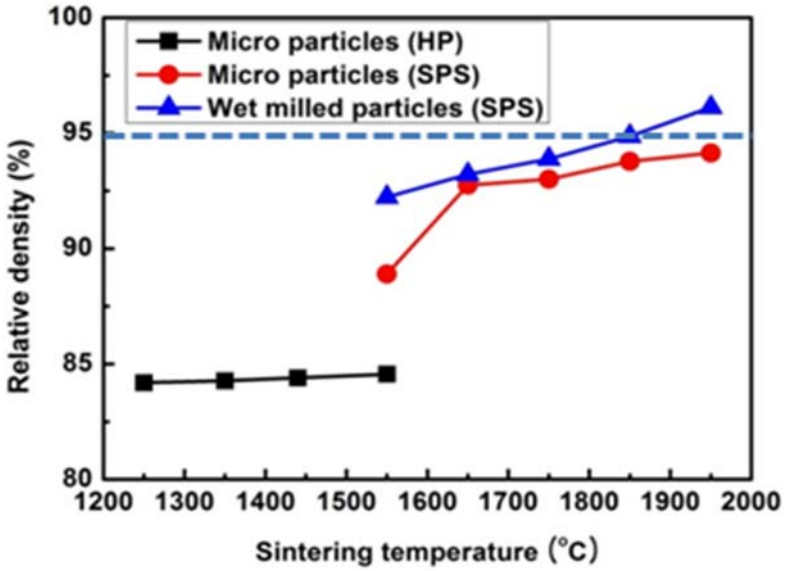

Figure Comparison of the relative density according to sintering process and feedstock particle

Keywords: tungsten, nano-attached particle, pulsed wire explosion, sinterability